UNITED NATIONS UNIVERSITY
UNU-GTP
Geothermal Training Programme

Orkustofnun, Grensasvegur 9,
IS-108 Reykjavik, Iceland

Reports 2014
Number 14

GAS - MINERAL EQUILIBRIUM IN THE BERLÍN GEOTHERMAL FIELD, EL SALVADOR

Jaime Alberto Hernández Ayala
LaGeo S.A. de C.V.
15 Av. Sur, Col. Utila
Santa Tecla, La Libertad
EL SALVADOR, C.A.
jhernandez@lageo.com.sv

ABSTRACT

The aquifer fluid composition at the depth of the volcanic geothermal system of Berlín, El Salvador, was reconstructed based on samples of steam and liquid from discharge fluids of 14 two-phase producer wells sampled during the period from July to October 2013 using the chemical speciation program WATCH 2.4. Berlín geothermal field is a liquid-dominated field with discharge enthalpies close to that of the reservoir liquid, except for well TR18B which has higher enthalpy because of phase segregation between the liquid and fluid phase in the depressuration zone around the well. The objectives of this study were to interpret deep fluid gas composition with the purpose of understanding gas behaviour in the geothermal system. The state of equilibrium between CO_2, H_2S and H_2 in the aquifer water and selected mineral assemblages that could potentially fix the concentrations of these reactive gases, in the temperature range from 200 to 300 °C, were studied. Field scale distribution of these gases, along with N_2, indicates that the H_2S and H_2 are temperature controlled; CO_2 follows a similar pattern in field scale distribution as N_2 which is a conservative gas in geothermal systems. Aquifer liquid H_2S concentration at the Berlin geothermal field is controlled by a close approach to equilibrium with the mineral assemblages. Hydrogen concentration for most of the wells lies close to equilibrium with the epidote-wollastonite-grossular-magnetite-quartz hydrothermal mineral assemblage. The aquifer concentration of CO_2 species was observed to fall below equilibrium with respect to the mineral buffers, suggesting that the concentration of the gas is source controlled.

1. INTRODUCTION

Two high-temperature geothermal fields are managed by LaGeo S.A. de C.V. in El Salvador, Ahuachapán geothermal field in the west part of the country and Berlín geothermal field in the east. Combined, these geothermal fields, with a total nominal installed capacity of 204.4 MWe, produce around 23% of the total electricity generation in El Salvador.

Electricity generation from the Berlín geothermal field began in 1992, when two 5 MWe back pressure power units went online. From 1997 to 1999, 8 producers and 10 injector wells were drilled in the field, a new 56 MWe (2 x 28 MWe) condensation unit was built and the previous two back pressure

units were disconnected. A new exploration project was carried out under the shareholder agreement Enel–GESAL (now LaGeo) to explore the southern part of the field and additional production wells were drilled during 2003 to 2005. Operation of Unit 3 (44 MWe condensation unit) started in 2007 and, in 2008, Unit 4, a 9.4 MWe combined cycle power plant was commissioned. The total installed capacity of this field is currently 109.4 MWe, which is equivalent to around 7% of the total install capacity of El Salvador, with a 13% contribution to national electricity production.

Since production at Berlín geothermal field was started in 1992, the reservoir response and management of field operations has been well documented and several studies related to geochemical interpretation of gases and aquifer fluid compositions have been made (D'Amore and Tenorio, 1999; Montalvo and Axelsson, 2000; Renderos, 2002; Jacobo, 2003; Ruggieri et al., 2006; Hernández, 2012). The role of gas geochemistry in assessing the reservoir becomes more relevant, especially in geothermal fields, with a long utilization history. A common consequence of long-term utilization is an increase in the vapour to liquid ratio in the discharges of producing wells due to reservoir pressure drawdown. Many geochemical processes affect the concentrations and ratios of reactive and unreactive gases in the fluids of volcanic geothermal systems. These processes may include a supply of gases from the magma heat source, from the atmosphere and from the water-rock interactions in the geothermal system. In gas geochemistry studies, the premise is the assumption of a close approach to equilibrium in the aquifer, either among specific reactive gases commonly present in geothermal well discharges or between some reactive gases and potential mineral buffers in the geothermal field. Due to the relatively high abundance and reactivity of the main geothermal gases (CO_2, H_2S and H_2), these components were viewed with particular interest in their ability to elucidate the physical nature of hydrothermal systems. Early studies provided compelling evidence that fluid compositions were controlled by equilibrium with select hydrothermal alteration minerals commonly identified in well cuttings, and many studies have shown that the aquifer fluid concentrations reactive geothermal gases closely approach equilibrium with specific hydrothermal mineral assemblages (Angcoy, 2010; Arnórsson et al., 2007, 2010; Karingithi et al., 2010; Scott, 2011).

In this study, an attempt is made to model the aquifer fluid composition in the Berlín geothermal field, using chemical data from water and steam discharge samples obtained from 14 production wells. Solute geothermometers were calculated and used to model aquifer fluid compositions and evaluate specific mineral-gas equilibria that may potentially control the concentrations of the reactive gases (CO_2, H_2S and H_2) in aquifer fluid in the geothermal reservoir. Such geochemical assessments provide insights on current reservoir conditions.

2. BERLIN GEOTHERMAL FIELD

The Berlin geothermal field is located about 110 km east of San Salvador, the capital city of El Salvador, in the district of Usulután, between the cities of Alegría and Berlín (Figure 1). It is located on the northern flank of the Berlín-Tecapa volcanic complex, inside a system of faults in the southern part of the east-west oriented Central American graben. The Berlín geothermal field is a volcanic liquid-dominated high temperature system (Saemundsson, 2009) with temperatures in the range of 280°C to 300°C in the central zone, and 240°C to 270°C in the southwest zone according to measured temperatures in the production wells.

A summary with information related to the geothermal production wells in operation at the Berlín geothermal field is presented in Table 1.

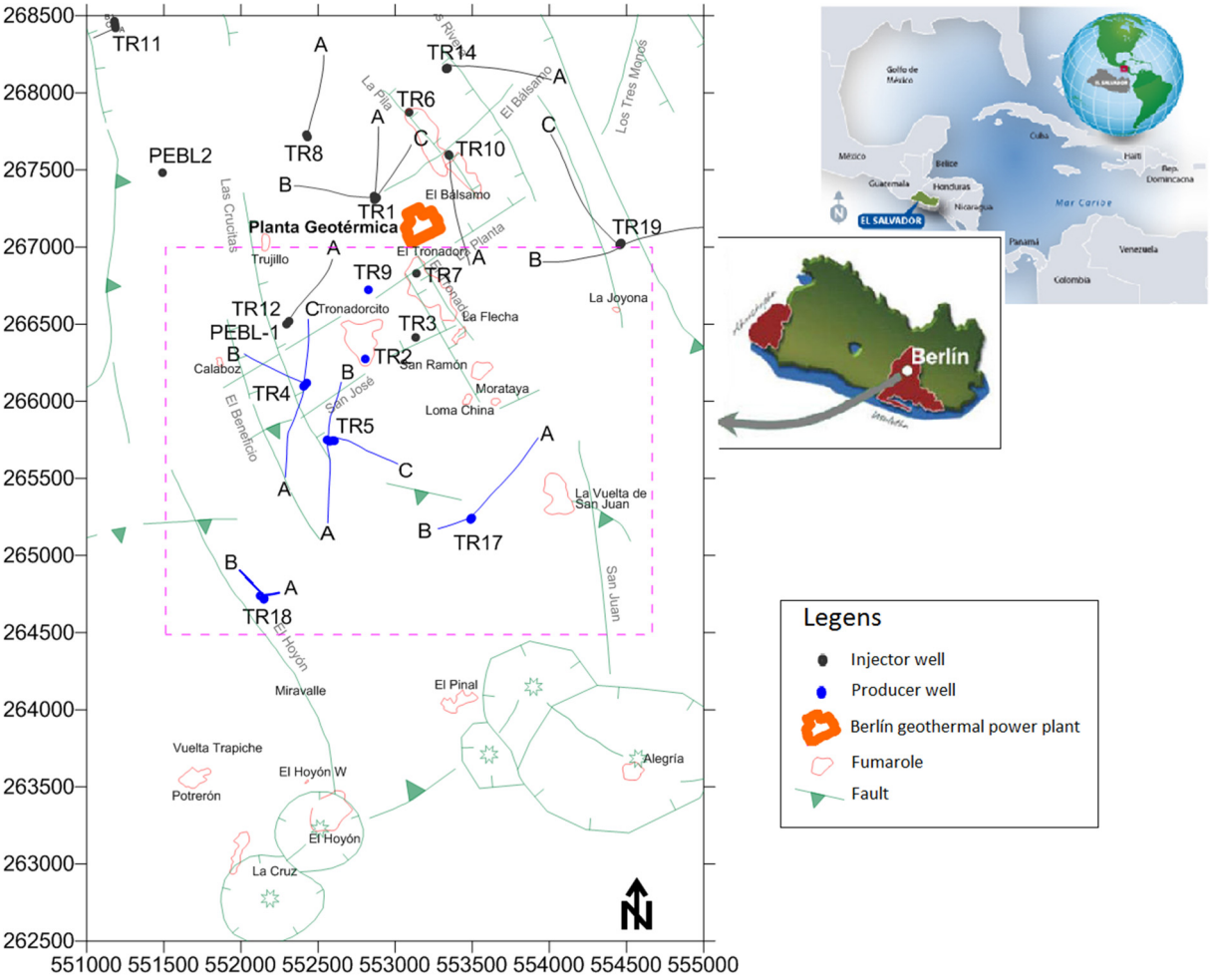

FIGURE 1: Berlín geothermal field: pink rectangle shows the spatial reference for field-scale distribution maps

2.1 Geological overview

High temperature geothermal activity in Central America is focused around plate subduction zones. El Salvador borders the Middle America Trench, an active subduction boundary and seismic zone between the Cocos and Caribbean plates. As a consequence, El Salvador is bisected by the volcanic front, a linear belt of active volcanoes and an accompanying seismic zone. The geologic and tectonic processes of both plate margins contribute directly to generating the main parameters for geothermal resources: heat and rock permeability. The volcanoes along the Central American volcanic arc supply the heat and the tectonic interactions between the plates generate the faults and seismicity that induces secondary permeability. Intense tropical precipitation contributes to the third parameter needed in a geothermal resource: geothermal fluids (Barrios et al., 2011).

Berlín geothermal field is categorized as a volcanic geothermal systems (Saemundsson, 2009). Associated with volcanic activity, Berlín geothermal power plants are located on the northern flanks of Holocene volcanoes with no history of eruptive activity in the past 500 years (Barrios et al., 2011). The heat sources for such systems are associated with magma chambers of the Berlín-Tecapa volcanic complex which was formed by the caldera of the Berlín strata volcano, and composed of a series of peripheral volcanic cones that expelled andesitic lava and scoria which emerge around the craters in the southeast part of the caldera of the old Berlín volcano (Correia et al., 1996). This volcanic complex is a stratovolcano composed of alternating lava flows, pyroclastics and andesitic epiclastites of

andesitic-basaltic nature. It is located inside the system of faults in the southern part of the E-W oriented Central American graben, in the zone of crustal weakness produced by the intersection of the NW-SE and NE-SW faults of the Central American graben.

TABLE 1: Summary of information on production wells in Berlín geothermal field

Well	Lambert projection[a] Northing Y	Lambert projection[a] Easting X	Elevation a.s.l. (m)	Condition deviation	Depth b.g.l. (m)	Circulation losses (m)	Temperature logging[b] (°C)	Finished Drilling (dd/mm/yyyy)	Started Production (dd/mm/yyyy)
TR2	266276	552802	752	VERT	1903	PL: ..805-1800 TL: 1799-1903	281	06/02/1978	02/20/2002
TR4	266098	552405	767	VERT	2379	PL: 1865-1948 TL: 1948-2379	280	07/08/1980	05/06/2011
TR4B	266270	552090	767	N-56-W	2292	PL: 1869-1892 TL: 1944-2292	294	03/30/1998	07/02/1999
TR4C	266450	552436	767	N-05-W	2179	PL: 1761-2179 TL: 1752	283	08/24/1998	01/02/1999
TR5	265744	552606	853	VERT	2086	PL: 1650-1830 TL: 1830-2086	301	07/04/1981	04/11/1999
TR5A	265250	552583	840	S-03-W	2325	PL: 1900-2000 TL: 2000-2194	296	08/29/1998	29/09/1999
TR5B	266073	552636	840	N-17-E	2097	PL: 1671-2000 TL: 2000-2097	297	12/31/1998	16/02/2000
TR5C	265590	552999	840	S-70-E	2343	PL: 1864-1996 TL: 1996-2343	301	03/23/1999	29/09/1999
TR9	266723	552826	649	VERT	2298	PL: 1448-1663 TL: 1663-2298	275	12/28/1980	01/01/1995
TR17	265243	553497	1073	VERT	2600	PL: -- TL: 1400-2000	253	12/01/2003	02/04/2007
TR17A	265709	553888	1073	N-36-E	2690	PL: 1750-1820 TL: 2000-2690	285	06/22/2004	05/13/2007
TR17B	265183	553300	1073	S-74W	1845	PL: -- TL: 1263-1845	269	01/03/2005	02/04/2007
TR18	264716	552149	995	VERT	2660	PL: -- TL: 1875-2660	266	02/25/2004	02/04/2007
TR18A	264760	552230	995	N-77-E	1085	PL: -- TL: ..929-1085	266	06/30/2004	02/04/2007
TR18B	264843	552055	1013	N-40-O	1194	PL: -- TL:.. 866-1194	240	09/24/2012	08/08/2013

[a]: coordinates for total lost-circulation zone in the well (WGS84/Zone 16N).
[b]: maximum temperature record on well logging

Two main active fault segments are recognized in the eastern part of El Salvador. A strike-slip system consists of mainly E-W faults, synthetic (WNW-ESE) and antithetic (NNW-SSE) Riedel shears, and NW-SE tensional structures. This last fault system, running NW-SE, is considered the most recent, active and important because it permits the ascent of the fluids from depth to the surface. The NNW-SSE fault system is the most important regionally as it is responsible for the formation of the Central American graben and also the active Quaternary volcanic chain of the country. Some of the most recent volcanic edifices such as Cerro Pelón, Laguna de Alegría and Cerro de Alegría, are aligned along the same course, indicating that this tectonic system is active and does not only exist in the Berlín zone, but in the whole country. This system has generated a graben that cuts through the northern part of this caldera. The majority of the hydrothermal manifestations and the geothermal field itself are found inside this structure (Correia et al., 1996).

This alkaline volcanic complex alternates basaltic to andesitic lava flows and scoria, and andesitic to dacitic ignimbrites which were produced during major eruptions (Raymond et al., 2005). Permeable fractures and fault zones, but also permeable strata such as ignimbrites and lavas, control the flow of water in this volcanic geothermal system.

2.2 Alteration mineralogy

Hydrothermal alteration of rocks and minerals is the result of chemical exchange that occurs during water-rock interactions between hydrothermal fluids (hot water) and the primary minerals and glass in the rock hosting the hydrothermal fluids. Primary minerals are replaced by secondary (alteration) minerals because the primary minerals are unstable in the fluid and secondary minerals are stable. Which types of alteration minerals are formed depends upon the geological setting, temperature and fluid properties in the system. Formation of alteration minerals may include the following processes: (1) transformation of mineral phases, (2) growth of new minerals, (3) dissolution and/or precipitation of minerals, (4) ion exchange reactions between rock minerals and fluid, etc.

The rocks intersected by geothermal wells in the Berlin geothermal field mainly consist of volcanic rocks and volcanic breccias. These rocks are always affected to a variable degree by hydrothermal alteration. Alteration of primary minerals occurs similarly in most geothermal fields, but some are specific to some fields. According to Ruggieri et al., (2010), four hydrothermal alteration zones, summarized in Table 2, have been recognized in the Berlin geothermal field, formed at increasing temperature and different depths: (1) from the surface to 670-700 m b.g.l., a relatively low temperature assemblage, consisting of clay minerals, heulandite, quartz and calcite occurs; (2) from 670-700 to 1100-1630 m b.g.l., the main hydrothermal phases are calcite, chlorite, quartz and a lesser amount of wairakite, laumontite, anhydrite, illite and illite-montmorillonite mixed-layers; (3) from 1100-1630 to 1460-1840 m b.g.l., epidote and albite occur together with most of the minerals of the previous hydrothermal assemblage; (4) below 1460-1840 m b.g.l., epidote, quartz and albite are the main hydrothermal phases while chlorite, actinolite, wairakite, adularia, prehnite, anhydrite and hydro-garnet occur in variable amounts.

TABLE 2: Hydrothermal minerals and depth ranges of the four alteration zones recognized in the Berlín geothermal field (Ruggieri et al., 2006)

Depth b.g.l. (m)		**Hydrothermal minerals**	
min	**max**	**Abundant**	**Moderately abundant to trace**
0	670-800	Nontronite, montmorillonite, corrensite, quartz, calcite, heulandite	Saponite
670-800	1100-1630	Calcite, chlorite, quartz	Wairakite, laumontite, anhydrite, illite, illite-montmorillonite, corrensite
1100-1630	1460-1840	Albite, quartz, chlorite, calcite	Illite, wairakite, adularia, prehnite, epidote
1460-1840	?	Epidote, albite, quartz	Adularia, prehnite, anhydrite, chlorite, actinolite, wairakite, hydro-garnet, calcite (Widespread titanite and pyrite without depth distribution)

Hydrothermal alteration minerals at Berlín geothermal field appear both as replacements of the primary minerals, as well as fillings in cavities or fractures crosscutting the rock. Figure 2 shows the distribution of the hydrothermal alteration zones at depth and the first appearances of minerals in the Berlín geothermal field. The abundance of the hydrothermal minerals and the alteration style are partially controlled by the bulk chemistry of the rock (Table 3). The shallowest alteration zone is characterized by the presence of relatively low-temperature minerals. At greater depth, hydrothermal phases, such as epidote, wairakite, prehnite, and hydro-garnets, typical of higher temperature conditions, occur. Quartz, calcite and chlorite are widespread in most of these zones (Ruggieri et al., 2006).

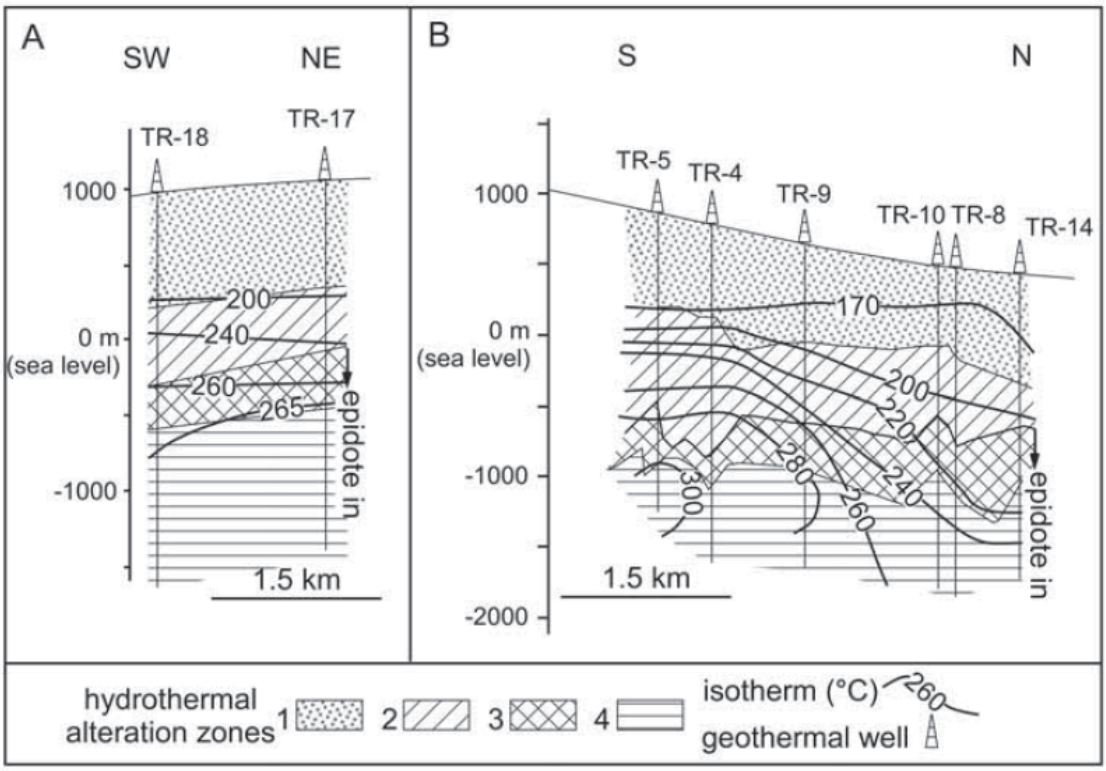

FIGURE 2: Distribution of the hydrothermal alteration zones with depth and the first appearances of minerals and corresponding subsurface temperatures indicated (reprinted from Ruggieriet al., 2006); Alteration zones are those reported in Table 2: particular characteristic minerals of each zone are: 1) calcite + clay minerals, 2) chlorite + calcite + quartz, 3) chlorite + calcite + quartz + albite ±epidote±prehnite, 4) epidote + quartz + albite±prehnite

TABLE 3: Primary minerals, order of replacements and alteration products of Berlín geothermal field

Order of replacement	Primary minerals	Alteration products
Increasing order ↑	Volcanic glass	Clays, zeolites, quartz, calcite
	Olivine	Clays, chlorite, Fe-oxides
	Pyroxene, amphiboles	Chloriite, illite, calcite, pyrite, actinolite, clays
	Ca-plagioclase	Calcite, epidote, quartz, sphene, illite/sericite, anhydrite, prehnite, wairakite
	Sanidine, orthoclase, microcline	Adularia, illite/sericite
	Magnetite	Hematite, pyrite, sphene
	Quartz	No alteration

2.3 Fluid chemistry

Berlin Geothermal reservoir is liquid-dominated, sub-boiling at depth with temperatures ranging up to 300°C. Three different types of aquifers have been identified: (1) a shallow low-salinity aquifer at a depth between 200 and 300 m a.s.l.; (2) an intermediate saline aquifer with temperature around 200°C and located around sea level; and (3) a deeper saline aquifer at a depth ranging from -800 to -1,800 m a.s.l with temperature around 300°C (Hernández, 2012). The bulk of the production from the field is from the depth of neutral and mature NaCl aquifers. The initial aquifer fluid has moderate Cl content

(from 2500 to 6500 mg/kg), low Fe and Mg (<1.0 mg/kg), low sulphates (<25.0 mg/kg) and slightly-acid to neutral pH (from 5.0 to 6.0); CO_2 levels varies from 200 to 1100 mg/kg (TR17A and TR4). The non-condensable gas content at these values corresponds to around 0.15 to 0.51%w/w.

2.4 Well discharge enthalpies

The samples in this study were obtained from 14 producing wells with total discharge enthalpies of about 1100 to 1700 kJ/kg (Table 4). Most of the well discharges have liquid enthalpy (i.e. the enthalpy of the discharged fluid is equal, or very close, to the enthalpy of steam-saturated liquid at the aquifer temperature). The productive zones in the well are mostly below 1700 m depth (b.g.l). According to Magaña (2012), the overburden pressure prevents extensive boiling of the fluid throughout the field typically induced by reservoir pressure drawdown; a thermodynamic equilibrium can be inferred in the initial aquifer fluid nourished geothermal wells in Berlín, based on values of total discharge enthalpy and initial aquifer enthalpy calculated using quartz, Na/K and Na/K/Ca geothermometers.

The discharge enthalpy in well TR18B is higher than the liquid enthalpy of the steam-saturated geothermal fluid. Well TR18B is the shallowest steam-saturated liquid well in Berlín geothermal field and, in later sections, it will be demonstrated that phase segregation primarily accounts for the discharge enthalpy of this well.

2.5 Conceptual model

Conceptual models are descriptive or qualitative models, not used for calculations. They are mainly based on geological information, both from surface mapping and the analysis of subsurface data, remote sensing data, results of geophysical surveying, information on the chemical and isotopic content of the fluid in surface manifestations and reservoir fluid samples collected from wells, information on temperature and pressure conditions based on analysis of available well logging data, as well as other reservoir engineering information (Axelsson, 2013).

The actual conceptual model of the Berlín geothermal field is based on the integration and interpretation of multi-disciplinary inputs from LaGeo's geoscientists (Figure 3).

The producing reservoir is related to the presence of a resistive deep aquifer with resistivity above 40 ohm-m in correspondence with the occurrence of prophylitic facie, whose formation temperature is in the range of 240 to 300°C (Monterrosa and Santos, 2013). It is estimated that the reservoir aquifer has a temperature range of between 250 to 310°C, according to measured temperatures in the production wells. Overlying the geothermal reservoir are two shallower aquifers. A groundwater aquifer close to the surface is recharged by local rain in the area, and a deeper aquifer of an intermediate temperature (150 to 200°C) is found around sea-level and is about 300 m thick (Montalvo and Axelsson, 2000).

The heat source is associated with an active magmatic chamber of the Berlín-Tecapa volcanic complex, which is mainly of andesitic nature, recently formed (<0.1 My) and, according to geophysical studies, housed at a depth of about 6 km. Fumaroles and hydrothermal activity south of the Berlín geothermal field are evidence of the magma chamber and its activity. Based on the distribution of well logging temperatures, quartz geothermometers, hydrogen gas anomalies and geo-volcanological studies, it is believed that there are 2 upflowing regions. The major natural outflow of the reservoir is towards the central and northwest area, located close to the production well pads of wells TR4 and TR5. The second upflow zone is to the south in the vicinity of wells TR17 and TR18. It is postulated that during upflow in this second region, the hot fluid is mixed with surface water from the inflow zone on the top of the volcanic complex and, as a result, the temperature of the geothermal fluid is lower compared to the fluid in the central upflow zone (LaGeo, 2012).

TABLE 4: Chemical analysis of water and steam samples from production wells at the Berlín geothermal field

Sample	Well	Date of sampling month/year	Discharge enthalpy kJ/kg	SP[a] bar-g	Aquifer temp. °C[b]	Liquid phase (ppm)														Ionic balance (CBE%)[e]	Vapor phase (mmol/kg)					
						pH[c]	SiO_2	B	Na	K	Mg	Ca	Al	Fe	F	Cl	SO_4	CO_2[d]	NH3		CO_2	H_2S	H_2	CH_4	N_2	O2
2013-1388	TR-2	10/2013	1171	9.4	284	5.90	746	118	3874	683	0.086	117	0.63	0.12	0.52	7048	14.7	2.55	0.45	1.9	0.696	0.213	0.014	0.0030	0.012	0.0002
2013-1373	TR-4	10/2013	1291	8.0	288	6.84	786	95	3222	594	0.019	58	0.47	0.01	1.02	5428	15.2	4.74	0.13	-1.5	1.329	0.259	0.018	0.0036	0.047	0.0002
2013-1374	TR-4B	10/2013	1316	11.1	281	7.05	718	82	2403	484	0.011	32	0.74	0.01	0.75	4257	12.4	12.4	0.19	0.9	1.940	0.153	0.019	0.0034	0.043	0.0002
2013-1375	TR-4C	10/2013	1290	11.0	275	6.86	678	121	3886	675	0.022	142	0.73	0.03	0.67	7164	19.6	7.2	0.29	2.3	1.49	0.24	0.017	0.0035	0.035	0.0002
2013-1164	TR-5	07/2013	1278	10.1	282	6.12	733	115	3536	712	0.059	57	0.43	0.03	0.48	6018	11.5	2.7	0.23	-1.4	1.08	0.29	0.016	0.0031	0.024	0.0002
2013-1378	TR-5A	10/2013	1216	10.2	272	6.75	663	97	2950	534	0.038	60	0.30	0.65	0.74	5380	18.5	4.2	0.16	2.4	0.91	0.22	0.012	0.0027	0.027	0.0003
2013-1379	TR-5B	10/2013	1182	10.2	295	6.31	816	140	4230	765	0.121	139	0.32	0.68	0.61	7947	13.2	2.6	0.42	3.2	0.86	0.19	0.012	0.0026	0.010	0.0001
2013-1163	TR-5C	07/2013	1193	11.0	275	6.08	681	132	3744	715	0.11	132	0.63	0.06	0.63	6840	12.4	2.6	0.21	1.4	0.99	0.24	0.013	0.0030	0.019	0.0005
2013-1380	TR-9	10/2013	1189	10.4	247	7.09	519	95	3110	487	0.011	156	0.64	0.03	0.82	5887	22.4	4.2	0.37	3.4	0.73	0.20	0.015	0.0030	0.014	0.0003
2013-1389	TR-17	10/2013	1141	6.9	277	6.04	719	129	4283	736	0.158	189	0.22	0.23	0.79	7650	10.2	2.6	0.21	0.3	0.85	0.15	0.004	0.0002	0.015	0.0002
2013-1390	TR-17A	10/2013	1156	7.3	244	7.10	517	123	4167	620	0.15	273	0.33	0.10	1.15	7636	25.5	3.1	0.22	1.2	0.49	0.11	0.001	0.0002	0.012	0.0001
2013-1391	TR-17B	10/2013	1101	7.5	281	6.70	742	131	4090	675	0.152	215	0.20	0.73	0.93	7564	17.8	2.6	0.18	1.9	0.60	0.10	0.001	0.0001	0.009	0.0001
2013-1407	TR-18	10/2013	1168	9.6	268	7.49	645	84	1875	308	0.011	34	0.99	0.04	0.76	3248	24.8	20.3	0.35	0.8	1.96	0.37	0.003	0.0005	0.056	0.0002
2013-1408	TR-18B	10/2013	1693	8.6	238	6.01	502	82	1911	332	0.011	71	0.92	0.09	3.48	3384	17.7	9.0	1.68	0.6	6.33	0.46	0.036	0.0006	0.089	0.0012
2013-1182	TR-18B	07/2013	1822	5.0	249	6.90	597	95	2348	383	0.279	148	2.92	1.06	4.81	4198	25.3	9.3	15.5	-0.1	2.56	0.44	0.016	0.0007	0.035	0.0011
2013-1208	TR-18B	07/2013	1748	5.0	244	6.65	566	107	2210	397	0.172	126	1.85	0.54	-	4209	26.5	12.8	6.83	2.9	4.79	0.71	0.016	0.0005	0.074	0.0006
2013-1236	TR-18B	08/2013	1680	11.9	235	5.94	470	88	2077	332	0.011	88	1.14	0.02	3.95	3516	24.2	13.0	3.25	-1.5	8.75	0.59	0.061	0.0008	0.131	0.0003
2013-1244	TR-18B	08/2013	1472	11.8	238	5.98	488	89	2118	353	< 0.01	89	0.94	0.13	4.42	3724	24.0	13.3	2.82	0.2	6.90	0.55	0.048	0.0006	0.101	0.0004
2013-1250	TR-18B	08/2013	1489	11.6	241	5.97	504	80	2094	347	< 0.01	84	0.92	0.09	3.99	3652	23.3	14.1	1.99	-0.1	7.18	0.49	0.054	0.0005	0.097	0.0006
2013-1409	TR-18B	10/2013	1693	8.7	237	6.04	495	90	1885	332	0.014	71	-	-	3.04	3438	18.3	9.4	1.25	1.9	6.64	0.46	0.031	0.0005	0.069	0.0002
2013-1549	TR-18B	12/2013	1150	9.0	234	6.21	476	89	2043	345	0.046	74	-	-	2.98	3653	22.6	14.0	-	1.3	7.25	0.46	0.048	0.0006	0.102	0.0004
2014-0066	TR-18B	01/2014	1653	9.5	241	6.06	516	85	2079	358	< 0.01	75	-	-	3.22	3629	24.1	14.0	0.83	0.0	7.86	0.45	0.049	0.0006	0.111	0.0019
2014-0217	TR-18B	02/2014	1652	9.2	241	6.39	516	97	2099	367	< 0.01	76	-	-	3.01	3595	26.5	16.9	1.07	-1.0	7.34	0.43	0.036	0.0004	0.084	0.0007
2014-0360	TR-18B	04/2014	1652	9.2	240	6.59	511	82	1958	313	< 0.01	70	-	-	3.45	3511	21.9	11.8	0.72	1.7	9.84	0.45	0.063	0.0008	0.146	0.0001
2014-0891	TR-18B	07/2014	1676	9.0	235	6.39	484	89	1989	316	< 0.01	68	-	-	2.61	3415	24.9	11.6	0.74	-0.4	8.33	0.43	0.054	0.0006	0.120	0.0002

[a]: SP: sampling pressure
[b]: temperature was based on the quartz geothermometer (Gudmundsson and Arnórsson, 2002)
[c]: pH was measured at laboratory using automatic temperature compensation (ATC) at 25°C
[d]: total carbonate carbon as CO_2
[e]: calculated according Equation 1

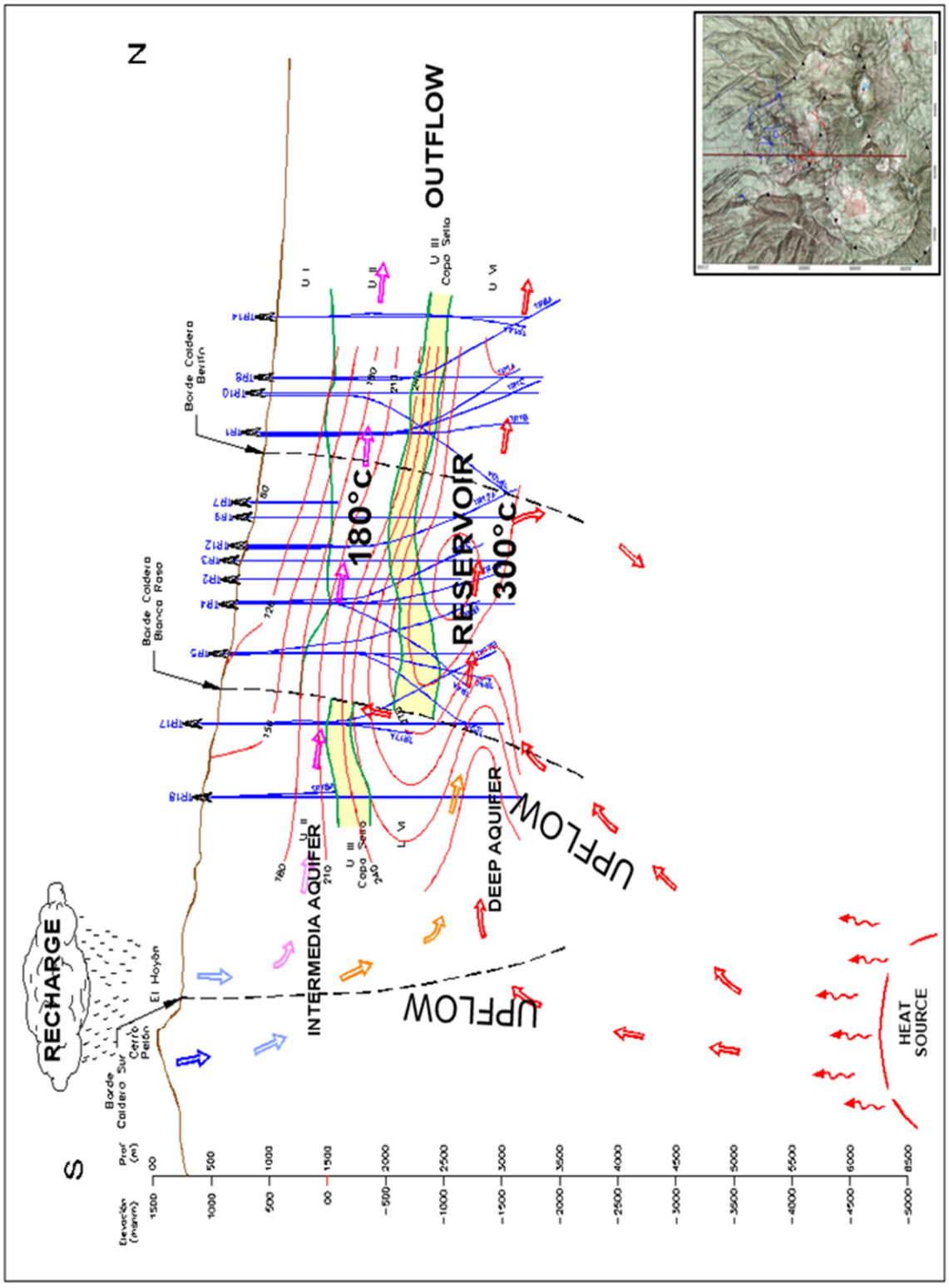

FIGURE 3: Vertical cross-section of the conceptual model of Berlín geothermal field (Monterrosa and Santos, 2013)

The geothermal fluid, consequently, flows through the main reservoir, moving from south to north or northwest along the NNW-SSE graben to reach the zone of well TR5. The upflow from the south moves to the northwest along the NW-SE system of faults El Hoyón, El Beneficio, Las Crucitas, San Juan y el Tronador to reach the central part where it changes course to the ENE-WSW, through the San José and La Planta faults. A tracer test carried out at Berlin geothermal field showed no flow between the reinjection zone (located in the north) and the production zone (Montalvo and Axelsson, 2000).The outflow of the systems is not known with any certainty but has been correlated with some of the hot springs located to the north (Monterrosa and Santos, 2013).

3. METHODOLOGY

Determination of the chemical composition of high temperature aquifer fluids involves sampling, treatment and chemical analysis of surface well discharge fluids and, secondly, the calculation of initial aquifer fluid chemical compositions.

This section describes the sampling and analysing methods used for the samples in this study. Aquifer chemical compositions were calculated from analysis of discharged water and steam phase using the chemical speciation program WATCH (Arnórsson et al., 1982; Bjarnason, 2010), version 2.4. A phase segregation model (Angcoy, 2010; Arnórsson et al., 2007, 2010; Karingithi et al., 2010; and Scott, 2011) was applied to calculate initial aquifer fluid composition in well TR18B after identification of the process which produced discharge enthalpies in excess of that of vapour-saturated liquid at the aquifer temperature for that well.

3.1 Sampling and physico-chemical analysis

The chemical composition of the deep water of a geothermal reservoir is a product of the source of water, water rock interactions and, in the case of volcanic environments, of magma degassing into the geothermal system. Chemical composition of geothermal fluid therefore provides important information about the characteristics of deep geothermal systems, which could be related with thermodynamic, geological and hydrological data. The accuracy and precision of the results obtained during integration of geochemical data are directly related to the quality of the chemical database which is dependent on using specific sampling techniques to achieve representative samples of the system under study, as well as qualified personnel, appropriate facilities and the use of appropriate analytical methods and instruments. Considering these needs, LaGeo geochemical laboratory has been accredited under ISO/IEC 17025 since 2003.

The primary data for this study were obtained from the water and gas discharges sampled during routine monitoring of 14 production wells in Berlín geothermal field. All fluids were sampled during the period from July to October 2013 except for samples collected from well TR18B which was sampled during the period from July 2013 to July 2014. Table 4 shows the chemical compositions of the water and steam samples used in this study.

Samples of water and steam for individual wells were collected at constant pressure; all the samples were collected and analysed by the geochemical laboratory of LaGeo. A chromium-nickel stainless (N316) steel Webre separator was connected in the two-phase pipeline by the wellhead to collect samples of water and steam. In some cases, samples were collected at separator stations. Water samples were cooled and steam was condensed using a stainless steel cooling coil prior to sampling. Condenser cooling was achieved using a 5-Gallon drum ice/water bath surrounding the coils. Calibrated Bourdon-tube type gauges were used for the measuring the sampling pressure.

Steam samples for non-condensable gas analysis were collected in duplicate into evacuated single stopcock valve gas bottles containing 50 ml of 4M NaOH solution. The strong base solution is used to capture the major non-condensable gases (CO_2 and H_2S) while residual gases (H_2, He CH_4, Ar, N_2 and O_2) occupy the head space of the gas bottle. Water samples for analysis of all components except for pH, total carbonate carbon, NH_4 and SiO_2, were filtered on site to prevent interaction with any suspended matter. The samples were treated in different ways, depending on the component to be analysed and the analytical methods; a general sampling procedure table specifying the treatment and sub samples for two-phase geothermal wells is shown in Table 5.

The non-condensable gases in the headspace of the gas sampling bulb (H_2, He CH_4, Ar, N_2 and O_2) were analysed by gas chromatography, while CO_2 and H_2S in the base solution were analysed by potentiometric titration. Total carbonate carbon concentration and pH in the liquid phase were

determined in the laboratory immediately upon return from the field (within 3–5 days) by potentiometric titration and a calibrated pH electrode, respectively. The major aqueous components were analysed by various methods: atomic absorption spectrometry (SiO_2, B, Na, K, Mg, Ca, Li, Al and Fe); spectrophotometry (SO_4); and ion selective electrode for F, Cl and NH_3.

TABLE 5: Sample treatment for determination of major chemical components in geothermal fluids according to sampling procedures in the geochemical laboratory of LaGeo

Phase	Treatment	Container	Specification	Analysis
Liquid	Filtered/filter membrane pore size *0.45* µm; 1.0 ml conc. HNO_3 (Suprapur)	250 ml HDPE bottles	FA[a]	B, Na, K, Mg, Ca, Li, Al and Fe
	Unfiltered, completely filled bottle, air-free	250 ml amber glass bottles	pH and total carbonate carbon	pH, T-CO_2/HCO_3
	Filtered/filter membrane pore size *0.45* µm	250 ml HDPE bottles	FU[b]	Cl, SO_4, F and EC[c]
	0.5 ml conc H_2SO_4	250 ml amber glass bottles	Ammonia	NH_3
	Dilution;10 ml of sample added to 90 ml of distilled, deionized water	100 ml HDPE bottles	Silica	Total and monomeric silica (SiO_2)
	Unfiltered	80 ml HDPE bottles	Isotopes	δ^2H, $\delta^{18}O$
Steam	None	80 ml HDPE bottles	Isotopes	δ^2H, $\delta^{18}O$
	Evacuated double port gas bottle containing 50 ml of 2N H_3BO_3	Sampling: approx. 300 ml double port bottle; Storage: 250 ml amber glass bottles	Ammonia	NH_3
	Evacuated single stopcock valve gas bottles containing 50 ml of 4M NaOH	Approx. 300 ml single stopcock valve gas bottles	Gas sample	CO_2 and H_2S in NaOH, residual gases in gas phase (H_2, He, CH_4, Ar, N_2 and O_2)

[a]: FA: filtered and acidified [b]: FU: filtered and unacidified [c]: EC: electric conductivity

3.2 Data handling

The chemical characteristic of the discharges fluid in production wells in the Berlín geothermal system was carried out by the geochemical laboratory of LaGeo. The total fluid from the wells was assumed to be representative of the deep brine in a liquid-dominated geothermal reservoir.

The pressure at which samples are taken is an important variable as it, together with the enthalpy of the discharging fluid determines the ratio between water and steam in the discharge. Samples were collected at pressures generally between 6.5 and 11.5 bar-g. As sampling conditions are different between wells, analytical results are not directly comparable because the distribution of component concentrations, both in water and steam, depend on the sampling pressure. For this reason, normalization of the chemical data is necessary before comparing individual wells or two samples from the same well. The chemical composition in water and steam for all the wells, except for well TR18B, was calculated at 10 bar-a vapour pressure (180°C) with the aid of the WATCH program using the data of total discharge enthalpy and sampling pressure. Quartz, Na/K and Na/K/Ca geothermometers were calculated. A single initial aquifer fluid temperature was chosen as a good approximation of the "real" temperature of the reservoir. Initial aquifer fluid compositions were computed using a reference temperature calculated in a previous step for reconstruction of the aquifer's initial composition.

In general, three different models are used in the evaluation of initial aquifer fluid composition or initial reservoir fluid (Arnórsson and Stefánsson, 2005a). The first model corresponds to an isolated system so boiling is adiabatic, where the enthalpy of the well discharge is that of the initial aquifer fluid. The second and third models correspond to closed and open systems, respectively; for both systems, the enthalpy of the well discharge is considered to be higher than that of the initial aquifer fluid and the reason for the excess enthalpy is either conductive heating of the aquifer fluid after depressuration boiling, or phase segregation of the two phases. In the case of conductive heating, the composition of the total discharge does not change as the net result is removal of water molecules along with some gas from the liquid phase to the steam phase. In the case of phase segregation the steam, after boiling starts some distance from the well, is preferably discharged from the well. Capillary forces between the liquid and surfaces of the minerals and rocks in the reservoir hinder the liquid phase from discharging from the well; the liquid phase stays behind in the reservoir. In this model, discharge enthalpies from such systems can be greatly in excess of the initial fluid enthalpy, and the composition of the total well discharge is different from that of the initial aquifer fluid, i.e. the total concentrations of dissolved solid components, such as silica, boron or chloride, calculated in the total discharge, strongly decrease with increasing discharge enthalpy.

For all the geothermal wells, except for well TR18B, the evaluation of the initial aquifer fluid compositions were calculated using Model 1 (Arnórsson and Stefánsson, 2005b). According to this model, the depth level of first boiling is within the well and the thermodynamic system is considered to be an isolated system, in which case boiling is adiabatic. In this model, it is a reasonable assumption to take the total well discharge composition to represent the initial aquifer fluid. No mineral precipitation or dissolution is assumed as the fluid is modelled from the aquifer to the surface. The calculation of initial aquifer fluid compositions for well TR18B which displays "excess" enthalpy, was calculated using the concepts applicable to the open system phase segregation model or Model 3 (Arnórsson et al., 2007, 2010).

3.3 Data quality analysis

Data quality verification is essential to ensure that the data is suitable for implementation of geochemical tools and the interpretation of data that helps answer questions about the geothermal system. Evidence about discrepancies or exceeded control limits should be investigated.

Two main criteria were used to set up data quality control. For quality analysis of chemical data of the steam phase, the O_2 content in samples was used; it was assumed that no O_2 was present in the geothermal gas. Samples with data values lower than one percent (<1.0%) of O_2 with respect to total Non-Condensable Gases (NCG) were accepted as normal; higher values providing evidence of the presence of oxygen indicated air contamination. In this case, the analyses could be corrected by subtracting the atmospheric component, as described by Zhen-Wu (2010).

For quality analysis of chemical data of the liquid phase, ionic balances or the percent of the charge balance error (CBE%) were used (Equation 1). When ionic compounds dissolve in water, they are dissociated into ions. The CBE% is the percentage difference between positive charges (cations) and negative charges (anions) in a water sample.

$$CBE\ \% = \left(\frac{\sum z_{cation} * m_{cation} - \sum z_{anion} * m_{anion}}{\sum z_{cation} * m_{cation} + \sum z_{anion} * m_{anion}}\right) \cdot 100\% \quad (1)$$

where z_i = Charge of an ion I;
m_i = Molal concentration of i (mol/kg).

The calculus of CBE% helps to determine water analysis accuracy, and is based on the principle of electro-neutrality which proposes that the sum in mmol/kg or meq/l of the cations must be equal to the sum of anions in a solution.

The purpose in checking the cation-anion balance in a water analysis is to validate the water analysis results. More than 5.0% difference in the cation-anion balance might imply that the analysis is not accurate or a major cation or anion was not considered in the CBE% calculation. It is important to note that WATCH's equation for CBE% calculus considers the average of the sum of the cations and anions; therefore, the CBE% limit using the WATCH program must be <10.0% approximately.

3.4 Selection of aquifer fluid reference temperature

For the liquid phase, four solute geothermometers were calculated: (1) sodium-potassium (Na/K) (Truesdell, 1976), (2) Na-K (Arnórsson et al., 1998), (3) sodium-potassium-calcium (Na/K/Ca) (Fournier and Truesdell, 1973), and (4) quartz geothermometer (Gudmundsson and Arnórsson, 2002). Geothermometer equations used in this study are presented in Table 6.

The Quartz geothermometer was selected for the reference temperature and was calculated using data from Table 4. The WATCH program was run using total discharge enthalpy and sampling pressure data. Quartz geothermometer temperature was calculated using total silica (as SiO_2) concentration in water initially in equilibrium with quartz after adiabatic boiling to 10 bar abs. vapour pressure. Data of aquifer temperatures and fluid enthalpy calculated from geothermometry are shown in Table 7.

TABLE 6: Geothermometer equations; valid in the range 0-350°C at P_{sat}

Geothermometer	Equation (T in ºC)	Source
Na/K[a]	$\frac{856}{0.857 + \log(\frac{Na}{K})} - 273.15$	(1)
Na/K[b]	$733.6 - 770.551 \cdot Y + 378.189 \cdot Y^2 - 95.753 \cdot Y^3 + 9.544 \cdot Y^4$	(1)
Na-K-Ca[c]	$\frac{1647}{\log\left(\frac{Na}{K}\right) + \beta \cdot \log\left(\frac{Ca^{0.5}}{Na}\right) + 2.24} - 273.15$	(1)
SiO_2[d]	$-132.2 + 0.036206 \cdot X + (55.865 \cdot 10^{-6}) \cdot X^2 - (2.699 \cdot 10^{-8}) \cdot X^3 + 128.277 \cdot \log(X)$	(2)

(1) Arnórsson (2000); (2) Gudmundsson and Arnórsson (2002).

[a]: Valid in the range from 100 to 275°C.

[b]: Y represents the logarithm of the molar Na^+/K^+ activity ratio at equilibrium with pure low-albite and pure microcline.

[c]: Concentrations are in mol/kg and β = 1/3 was used.

[d]: X represents total silica (as SiO_2) concentration in water initially in equilibrium with quartz after adiabatic boiling to 10 bar abs. vapour pressure (180°C).

The Na/K geothermometer, according to Arnórsson et al. (1998), is based on feldspar solubility constants. The Na/K geothermometer of Truesdell (1976) was used for comparison of results between both Na/K geothermometers. The results were generally very close, in most cases within +/- 3.0°C.

The Na/K geothermometer shows a systematic discrepancy, with significantly lower temperatures than those given by the quartz geothermometer. According to Gudmundsson and Arnórsson (2002), this discrepancy is due to faulty calibration of the former geothermometer or partial re-equilibration in the depressurization zone around the discharging well. A new water-rock chemical equilibrium is attained in reservoirs where water resides for short periods of time, and the process of chemical re-equilibrium is faster for quartz than Na/K. The differences in temperature between Na/K, and Na/K/Ca, compared with the quartz geothermometer, was between 2 and 33°C, and are very close in wells TR4B, TR5, TR5A, TR5C, TR9 and TR17A; in most cases, the differences were minor, 10.0°C between Na/K and quartz; and 5.0°C between Na/K/Ca and quartz. Initial aquifer temperatures derived from geothermometry were compared with temperatures measured downhole in wells TR2, TR4, TR4C, TR5B, TR18 and TR18B.

TABLE 7: Aquifer temperatures and fluid enthalpy calculated from geothermometry

Sample	well	$h^{d,t}$	$h^{f,tlog}$	$h^{f,tqtz}$	Aquifer temperature (°C)					Aquifer temperature differences (°C)	
		(kJ/kg)			T_{log}[a]	T_{qtz}[b]	$T_{Na/K}$[c]	$T_{Na/K}$[d]	T_{NaKCa}[e]	T_{qtz} - T_{log}	T_{qtz} - T_{NaKCa}
2013-1388	TR2	1171	1241	1255	281	284	259	258	265	2.6	18.4
2013-1373	TR4	1291	1236	1277	280	288	264	265	273	7.9	15.2
2013-1374	TR4B	1316	1310	1242	294	281	275	278	280	-12.8	0.7
2013-1375	TR4C	1290	1251	1209	283	275	257	256	262	-8.2	12.9
2013-1164	TR5	1278	1349	1248	301	282	275	278	283	-18.6	-0.3
2013-1378	TR5A	1216	1321	1193	296	272	262	262	269	-24.4	2.8
2013-1379	TR5B	1182	1327	1314	297	295	262	262	267	-2.3	27.4
2013-1163	TR5C	1193	1349	1211	301	275	269	270	269	-25.7	6.2
2013-1380	TR9	1189	1210	1074	275	247	246	242	248	-27.6	-0.2
2013-1389	TR17	1141	1101	1218	253	277	256	255	259	23.6	17.2
2013-1390	TR17A	1156	1262	1058	285	244	240	235	244	-40.9	0.2
2013-1391	TR17B	1101	1180	1240	269	281	252	249	254	11.9	27.1
2013-1407	TR18	1168	1165	1175	266	268	251	248	257	2.1	10.9
2013-1408	TR18B	1693	1039	1029	240	238	257	256	252	-2.0	-14.0

$h^{d,t}$: Total discharge enthalpy;
$h^{f,tlog}$: Fluid enthalpy calculated using maximum temperature recorded on well logging;
$h^{f,tqtz}$: Fluid enthalpy calculated using quartz geothermometer temperature;
[a]: Maximum temperature recorded on well logging;
[b]: Temperature was based on quartz geothermometer (Gudmundsson and Arnórsson, 2002);
[c]: Temperature based on Na/K geothermometer (Arnórsson et al., 1998);
[d]: Temperature based on Na/K geothermometer (Truesdell, 1976);
[e]: Temperature based on Na/K/Ca geothermometer (Fournier and Truesdell, 1973).

3.5 Aquifer fluid composition modelling

The calculation of chemical composition of fluid in isolated boiling system (adiabatic boiling) is based on the conservation of mass and energy; under conditions where water and steam samples are collected at the same pressure (P^s), Equation 2 gives the concentration of chemical component *i* in the initial aquifer fluid of a wet-steam well (Arnórsson, 2008):

$$m_i^{d,t} = m_i^{f,l} = m_i^{d,l}\left(1 - X^{d,v}\right) + m_i^{d,v} \cdot X^{d,v} \quad (2)$$

where $m_i^{d,t}$ = Concentration of component *i* in total discharge;
$m_i^{f,l}$ = Concentration of component *i* in the initial aquifer fluid;
$m_i^{d,v}$ = Concentration of component *i* in vapour discharge;
$m_i^{d,l}$ = Concentration of component *i* in liquid discharge;
$\boldsymbol{X^{d,v}}$ = Vapour fraction in the discharge at vapour pressure Ps (by mass).

For components that partition almost exclusively in the liquid phase, at P^s, $\boldsymbol{m_i^{d,v}}$is taken to be zero by the WATCH program, and for gaseous components that are present in insignificant concentrations in liquid samples, therefore not analysed, $\boldsymbol{m_i^{d,l}}$ is taken to be zero. The steam fraction of a well discharge is given by Equation 3:

$$X^{d,v} = \frac{h^{d,t} - h^{d,l}}{h^{d,v} - h^{d,l}} \quad (3)$$

where $h^{d,t}$ = Total discharge enthalpy (kJ/kg);
$h^{d,l}$ = Liquid discharge enthalpy (kJ/kg);
$h^{d,v}$ = Vapour discharge enthalpy (kJ/kg).

It is important to note that to determine the steam to water ratio in a wet steam well discharge at a specific pressure, it is necessary to know the total discharge enthalpy from measurements.

3.5.1 Phase segregation model

According to the phase segregation model (Model 3), the thermodynamic system is considered an open system. This model assumes that the steam phase moves preferentially into the well while water is retained in the aquifer due to capillary forces between the liquid and surfaces of the rock and minerals in the feed zones of the well. This process causes changes in the discharge enthalpy and the chemical composition of the well discharge to differ from those of the initial aquifer fluid. The use of the phase segregation model in this study involves several assumptions: (1) an excess of enthalpy is due to phase segregation only; (2) phase segregation occurs at a specific vapour pressure (P^g); and (3) that the vapour fraction in the initial aquifer fluid is zero.

The pressure at which phase segregation occurs affects the calculated composition of the initial aquifer fluid. It is considered likely that phase segregation occurs over a pressure interval between the aquifer pressure and the vapor pressure of the fluid entering the well rather than at a single pressure.

In general, the initial aquifer fluid composition calculations, using the phase segregation model, involve two steps after constituting the aquifer temperature and the aquifer vapour pressure. The first consists of calculating the liquid and steam composition from discharge data (chemical composition of water and steam and discharge enthalpy) at the phase segregation pressure (P^g) at which phase segregation is assumed to occur. The second step involves calculating the initial aquifer composition from the fluid compositions at P^g, assuming that the enthalpy before phase segregation occurred is the same as that of the vapour-saturated liquid at the aquifer temperature (Giroud, 2008).

For well TR18B, P^g was calculated as follows:

- chemical data was calculated at 10 bar-a vapour pressure (180°C); the WATCH program was run using total discharge enthalpy and sampling pressure data;
- quartz geothermometer (t_{qtz}) temperature from Gudmundsson and Arnórsson (2002) was calculated using calculated silica concentration at 180°C;
- reservoir pressure (P^R) was calculated using t_{qtz} and steam tables;
- P^g was calculated as a midway pressure between wellhead pressure (WHP) and P^R.

Phase segregation temperature (T^e) was calculated using P^g and steam tables. Intermediate aquifer fluid compositions were calculated using T^e as the reference temperature; the WATCH program was run using total discharge enthalpy and sampling pressure data.
The initial aquifer fluid compositions were calculated using chemical data from Table 4: P^g was the sampling pressure, t_{qtz} was the reference temperature and the pH of the fluid was calculated at T^e.

Equation 2 can be rewritten and the concentration of chemical component *i* in the initial aquifer fluid calculated as follows:

$$m_i^{f,t} = m_i^{g,l}(1 - X^{e,v}) + m_i^{g,v} \cdot X^{e,v} \quad (4)$$

where $m_i^{f,t}$ = Concentration of component *i* in initial aquifer fluid;
$m_i^{g,v}$ = Concentration of component *i* in vapour discharge;

$m_i^{g,l}$ = Concentration of component *i* in liquid discharge;
$\boldsymbol{X^{e,v}}$ = Vapour fraction after depressurization boiling to P^g before retention of liquid in the aquifer.

As before for non-volatile species, $\boldsymbol{m_i^{g,v}}$ is taken to be zero. Equation 5, given the vapour fraction $\boldsymbol{X^{e,v}}$ at phase segregation pressure (P^g), is as follows.

$$X^{e,v} = \frac{h^{f,l} - h^{e,l}}{h^{e,v} - h^{e,l}} \quad (5)$$

where $\boldsymbol{h^{f,l}}$ = Initial aquifer fluid liquid enthalpy (based on reference temperature) (kJ/kg);
$\boldsymbol{h^{e,l}}$ = Intermediate zone liquid enthalpy at phase segregation pressure P^g (kJ/kg);
$\boldsymbol{h^{e,v}}$ = Intermediate zone vapour enthalpy at phase segregation pressure P^g (kJ/kg).

Chemical component concentrations in the initial aquifer fluid of well TR18B, were calculated by the method just described.

3.5.2 Evaluation of processes leading to excess discharge enthalpy in well TR18B

When the discharge enthalpy of a well exceeds that of steam-saturated water at the aquifer temperature (which is the case in well TR18B), it is referred to as displaying "excess" enthalpy. As previously mentioned, a different model needs to be selected to explain the cause of elevated well enthalpy. There are two most common processes that can lead to excess discharge enthalpy. The first one is conductive heat transfer from the aquifer rock to the fluid flowing through the depressurization zone around discharging wells; the second one is due to phase segregation or relative permeability of liquid water and vapour leading to their partial or total separation (Karingithi et al., 2010). Additionally, excess enthalpy may be due to the presence of steam in the initial aquifer fluid. However, the effects of conductive heat transfer or phase segregation, or both, generally seem to be more important (Arnórsson et al., 2007).

Measurements of the total discharge enthalpy of well TR18B are in the range of 1500 to 1800 kJ/kg. Liquid discharge enthalpy calculated by using quartz geothermometer temperature and logging temperature provide values of around 1050 kJ/kg.

To identify the processes leading to the excess of discharge enthalpy in well TR18B, the two processes mentioned above were taken into account. Cl concentration in the total discharge, and evaluation of the relationship between Na/K and quartz geothermometers, using the concentration of chemical species in the total discharge, were used. According to Arnórsson et al. (2007), if the concentration of a non-volatile, conservative component like Cl in the total discharge of a well stays about constant, despite variations in excess discharge enthalpy, the cause of the excess enthalpy is due to conductive heat transfer from the aquifer rock to the flowing fluid. As already indicated, it is reasonable to assume that the system is isolated since conductive heat transfer from the aquifer rock to the fluid increases the relative proportion of steam without affecting the total two phase fluid composition, i.e. the enthalpy and total well discharge composition remains the same as that of the initial aquifer fluid. On the other hand, if the excess enthalpy is due to phase segregation, Cl concentration in the total discharge approaches zero as the discharge enthalpy approaches that of saturated steam.

Calculated Cl concentration in the total discharge (Figure 4) shows that the concentration of Cl decreases with increasing enthalpy, and approaches zero at the enthalpy of pure steam. Quartz geothermometer temperatures together with the Na/K temperature were calculated according to both conductive heat transfer and phase segregation models for well TR18B (Figure 5).

The calculated temperature according to the Na/K geothermometer is not affected by either model, but the calculated quartz geothermometer temperature is affected by which model is used. When using the conductive heat transfer model, the calculated quartz temperature is systematically lower than the Na/K temperature and the difference increases with increasing discharge enthalpy. This result indicates that phase segregation is the dominant cause of excess discharge enthalpy in well TR18B. Model 3 (Arnórsson et al., 2007, 2010) was, therefore, used to calculate the initial aquifer fluid composition for the well.

3.6 Mineral equilibria and thermodynamic data

Thermodynamics gives a qualitative means of calculating the stable relationships between various phases of various compounds or combinations of compounds (mineral assemblages). The fact that a mineral assemblage changes into a different assemblage means that the new association has a lower free energy than the old at a given pressure and temperature and mineral association of all the alternative phases. Although a geothermal system, as a whole, is an open system with continual inflow and outflow of mass and heat, thermodynamics consider the geothermal reservoir as a bulk of small systems in equilibrium behaving locally as closed system. According to this model, the chemical composition of fluids in the geothermal reservoir approaches equilibrium with respect to several alteration minerals.

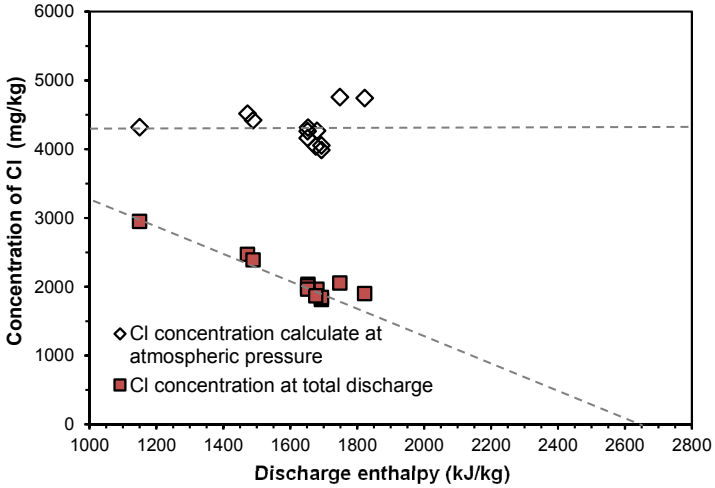

FIGURE 4: Relationship between Cl and discharge enthalpy in Well TR18B; Cl concentration in the total discharge approaches zero as the well discharge enthalpy approaches that of dry steam; this relationship further supports the theory that phase segregation is the cause of excess well discharge enthalpy in Well TR18B

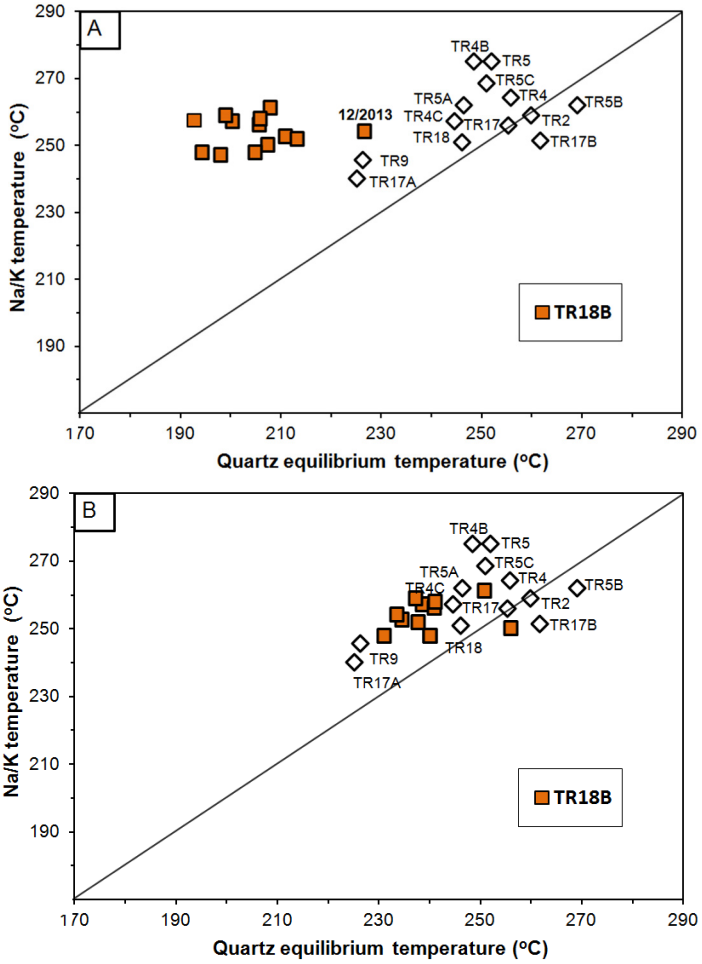

FIGURE 5: Relationship between Na/K and quartz geothermometers: Quartz equilibria temperature was calculated using the concentration of chemical species in total discharge according to conductive heat transfer (Model A) and phase segregation (Model B) for Well TR18B

The application of thermodynamics is an attempt to model local mineral equilibria that could potentially control the gas partial pressures in the reservoir. The calculus of equilibria between minerals, gases and liquid involve knowing the concentration of gases in equilibrium with the mineral assemblage and the activity of the species involved in the geothermal fluid. In this study, the concentration and activities of aqueous species were obtained with the aid of the WATCH program and several assumptions were made: (1) ideal behaviour in the mineral solid solution, (2) no vapour present in the initial liquid aquifer, and (3) unit activity for all minerals (anhydrite, calcite, hematite, magnetite, pyrite, pyrrhotite, quartz and wollastonite), except for epidote and prehnite solid solutions.

Data from selected microprobe analysis and structural formulae of epidote and prehnite from well core samples of the Berlin geothermal field reported by Ruggieri et al. (2006) was used to calculate the activities of end-members in epidote [$Ca_2Al_2FeSi_3O_{12}(OH)$] and prehnite [$Ca_2Al_2FeSi_3O_{10}(OH)_2$]. Primary data, given in weight percent oxide and the calculated chemical formula and end-member activity for each individual mineral analysis, as well as the average, are provided in Table 8. The average activities of end-member epidote and prehnite were calculated to be 0.72 and 0.66, respectively, resulting in a clinozoisite activity of 0.28. These values are similar to the average compositions in other geothermal systems (Arnórsson et al., 2010; Karingiti et al., 2010; Scott, 2011).

Most epidote solid solutions in geologic systems fall within the compositional range between clinozoisite and epidote, 2 common end-member components of epidote solid solution.

$[Ca_2Al_3Si_3O_{12}(OH)]$	$[Ca_2AlFe_2Si_3O_{12}(OH)]$	$[Ca_2Al_2FeSi_3O_{12}(OH)]$
clinozoisite	Pistacite	epidote

Ferric iron can occupy the M1 and M3 sites. The activity composition relationships for epidote and clinozoisite were calculated according to Freedman et al. (2010), using data from Table 8. Mineral buffer reaction equilibrium between dissolved H_2S, CO_2 and H_2 is plotted against the mineral assemblages that could potentially fix the concentrations of these reactive gases (see later in Figure 7). The equilibrium curves for the gas-mineral assemblages are based on the respective equations for the end-member minerals according to thermodynamic data for H_2S, CO_2 and H_2 as given by Arnórsson et al. (2010). The log k-temperature equations and the reactions for which equilibrium constant curves have been drawn are listed in Table 9. The activities in the solid solution minerals were taken into account for the elaboration of each equilibrium curve. To explain this further, consider reaction 6 in Table 9.

TABLE 8: Results of microprobe analysis and structural formulae of epidote and prehnite from well core samples of the Berlin geothermal field (modified from Rugierri et al., 2006)

	Weigh percent oxide								Chemical formula	
Well	**SiO_2**	**Al_2O_3**	**CaO**	**FeO**	**SUM**	**n_{Fe}**	**n_{Al}**	**$X_{Fe,M3}$**	**Unit formula epidote**	**a_{epi}**
TR-5B	38.57	26.10	23.66	9.68	98.01	0.63	2.38	0.21	Ca1.96Al1.04Fe0.63Si2.99O12.5(OH)	0.63
TR-8A	38.04	22.00	23.38	15.03	98.45	0.99	2.03	0.33	Ca1.97Al1.13Fe0.99Si2.99O12.5(OH)	0.77
TR17A	38.67	26.58	23.40	10.48	99.13	0.67	2.40	0.22	Ca1.92Al1.56Fe0.671Si2.95O12.5(OH)	0.66
TR-18	37.89	22.50	22.61	16.19	99.19	1.05	2.06	0.34	Ca1.88Al1.93Fe1.05Si2.94O12.5(OH)	0.81
								Average:	Ca1.94Al2.29Fe0.76Si2.97O12.5(OH)	0.72
Well	**SiO_2**	**Al_2O_3**	**CaO**	**FeO**	**SUM**	**n_{Fe}**		**$X_{Fe,Prehnite}$**	**Unit formula prehnite**	**a_{Pre}**
TR-17	43.6	20.9	26.07	3.84	94.41	0.43		0.43	Ca3.92Al1.57Si6.12O20(OH)2	0.57
TR-17	38.8	25.4	23.04	9.21	96.45	0.26		0.26	Ca3.50Al1.74Si5.50O20(OH)2	0.74
								Average:	Ca3.71Al1.66Si5.81O20(OH)2	0.66

TABLE 9: Log K-temperature equations for the equilibrium constants for pure mineral and reactions for mineral assemblage reactions that may control the gas concentrations in a reservoir; data valid in the range from 0 to 350°C, at Psat; Source of thermodynamic data used to obtain the temperature equations is outlined by Karingithi et al. (2010)

#	Species	Equilibrium reaction for the gas mineral assemblages
1	CO_2	$czo + cal + \frac{3}{2}\,qtz + H_2O = \frac{3}{2}pre + CO_{2,aq}$
2	CO_2	$\frac{2}{5}czo + cal + \frac{3}{5}qtz = \frac{3}{5}gro + \frac{1}{5}H_2O_l + CO_{2,aq}$
3	H_2S	$\frac{1}{3}pyr + \frac{1}{3}pyrr + \frac{2}{3}pre + \frac{2}{3}H_2O_l = \frac{2}{3}epi + H_2S_{aq}$
4	H_2S	$\frac{1}{4}pyr + \frac{1}{2}pyrr + H_2O_l = \frac{1}{4}mag + H_2S_{aq}$
5	H_2S	$\frac{2}{3}gro + \frac{1}{3}pyr + \frac{1}{3}pyrr + \frac{2}{3}qtz + \frac{4}{3}H_2O_l = \frac{2}{3}epi + \frac{2}{3}wol + H_2S_{aq}$
6	H_2S	$2gro + \frac{1}{4}pyr + \frac{1}{2}mag + 2qtz + 2H_2O_l = 2epi + 2wol + H_2S_{aq}$
7	H_2	$\frac{4}{3}pyrr + \frac{2}{3}pre + \frac{2}{3}H_2O_l = \frac{2}{3}epi + \frac{2}{3}pyrr + H_{2,aq}$
8	H_2	$\frac{2}{3}pyr + H_2O_l = \frac{3}{4}pyr + \frac{1}{4}mag + H_{2,aq}$
9	H_2	$\frac{2}{3}gro + \frac{4}{3}pyrr + \frac{2}{3}qtz + \frac{4}{3}H_2O_l = \frac{2}{3}epi + \frac{2}{3}wol + \frac{2}{3}pyr + H_{2aq}$
10	H_2	$6gro + 2mag + 6qtz + 4H_2O_l = 6epi + 6wol + H_{2,aq}$
#	**Species**	**log K-temperature equations (°K)**
1	CO_2	$-0.890 + 7251.5/T^2 - 1710.6/T + 0.004188T + 0.000002683T^2 - 0.064\log T$
2	CO_2	$-1.449 - 40536/T^2 - 2135.9/T + 0.0065639T + 0.000002725T^2 - 0.193\log T$
3	H_2S	$13.608 + 592324/T^2 - 9346.7/T - 0.043552T + 0.000029164T^2 + 5.139\log T$
4	H_2S	$13.659 + 555082/T^2 - 9256.6/T - 0.043608T + 0.000028613T^2 + 5.148\log T$
5	H_2S	$-0.836 - 216659/T^2 - 2847.3/T + 0.008524T - 0.000002366T^2 + 0.152\log T$
6	H_2S	$13.589 + 590215/T^2 - 9024.5/T - 0.044882T + 0.000029780T^2 + 5.068\log T$
7	H_2	$-1.640 - 124524/T^2 - 777.19/T - 0.0005501T + 0.000007756T^2 - 0.565\log T$
8	H_2	$-1.544 - 151109/T^2 - 752.389/T - 0.0005868T + 0.000007080T^2 - 0.532\log T$
9	H_2	$1.444 - 273812/T^2 - 3962.1/T + 0.002401T + 0.0.000001304T^2 - 0.979\log T$
10	H_2	$-1.654 - 95456.8/T^2 - 621.84/T - 0.001257T + 0.000007569T^2 - 0.600\log T$

$$2\text{gro} + \frac{1}{4}\text{pyr} + \frac{1}{2}\text{mag} + 2\text{qtz} + 2\text{H}_2\text{O}_\text{l} = 2\text{epi} + 2\text{wol} + \text{H}_2\text{S}_\text{aq} \quad (6)$$

Taking the activities of grossular (gro) and epidote (epi) to be equal to 0.3 and 0.72, respectively, and taking the activities of pyrite (pyr), magnetite (mag), quartz (qtz), wollastonite (wol) and water (H_2O_l) to be equal to unity we have:

$$\log \text{K} = 2\text{epi} + \text{H}_2\text{S}_\text{aq} - 2\text{gro} \quad (7)$$

$$\log [\text{H}_2\text{S}] = \log \text{K} - 2\log(0.72_\text{epi}) + 2\log(0.3_\text{gro}) \quad (8)$$

The equilibrium curves for the gas-mineral assemblages were done using the log K-temperature value for each reaction and calculating the concentration of dissolved reactive gas (each 5°C) in the range from 200 to 300°C (473 to 513°K).

4. RESULTS AND DISCUSSION

4.1 Aquifer fluid composition

Information on the initial aquifer fluid chemical composition from Table 10 was used to study the distributions of reactive and conservative elements, both volatile and non-volatile, in the Berlin geothermal field. Field-scale distributions using "natural neighbour" together with "radial funct" gridding methods are shown in Figure 6.

Figure 6a shows the field-scale distribution of quartz equilibrium temperature in the Berlín geothermal field. The quartz geothermometer distribution suggests the flow moves along the NW-SE graben with the maximum temperatures in well pads TR4 and TR5 in the central and northwest part of the field. Quartz geothermometer temperatures were compared with temperatures measured downhole in wells TR2, TR4, TR4C, TR5B, TR18 and TR18B. Temperatures inferred from geothermometry were generally very close to the measured maximum temperature in the well in most cases, within +/-. 5.0°C. The discrepancy in some of the wells may be due to the aquifer in the wells producing at different horizons than what corresponds to where maximum temperature in the well is measured during well logging. Discharged fluid is usually a mixture of water from different feed zones in the well and the analysis of the discharge yields a weighted average composition of the feed zones

Figure 6b shows the field-scale distribution of Cl. The distribution shows an increase in the Cl concentration in the aquifer fluids from the west to the east with the higher concentrations in the zone of the production well pad TR17. Quartz geo temperatures are higher (>10.0°C) than the maximum temperatures measured downhole in wells TR17 and TR17B. According to Magaña (2012), wells TR17 and TR17B are in equilibrium with wairakite and suggest the possibility of evaporation for adiabatic expansion of the fluids in this zone. Higher Cl concentration in the east part of the field could be caused by boiling and steam loss of the fluids. This is in agreement with the N_2 and H_2 depletion in the fluids in that part of the field (Figures 6d and 6e). Moreover, the main source of Cl in the aquifer fluids is progressive dissolution of the host rock; the high concentration of Cl in well TR17 could indicate the deepest fluid feed zone. In contrast, well TR18B shows the lowest Cl concentration, lowest temperature, high N_2 content and strongly suggests a possible interaction (mixing and boiling process) among the geothermal fluid and recharging meteoric waters coming from the south. According to Scott (2011), a large depletion in H_2, relative high N_2 content and low Cl concentration, which is the case of well TR18B, could be evidence of cold recharge.

The distributions of CO_2 and N_2 on the scale of the geothermal field are shown in Figures 6c and 6d, respectively. As can be seen in both figures, they appear to follow similar patterns. N_2 is generally known to be conservative in geothermal fluids and its concentration in the fluid is, therefore, source controlled. The similar pattern in the field scale distribution in the geothermal field, therefore, indicates that CO_2 might also be source controlled. In the case of the former, its source is dissolution of basaltic rock, magma degassing or the dissolution of hydrothermal calcite precipitated in an earlier stage of the geothermal system; for the latter, the source is recharging air-saturated meteoric water or the CO_2 is degassed into the system from melting oceanic crust. Concentrations in aquifer fluids can also be affected by degassing prior to entering the producing zone of a well.

The field scale distributions of H_2 and H_2S are shown in Figures 6e and 6f, respectively. Especially for H_2S, the highest concentrations of these gases are calculated in the proximity of the proposed upflow zones, where the highest temperatures are found. The concentrations of H_2S and H_2 appear to follow similar patterns as the quartz geothermometer indicated: the concentrations of these gases are temperature controlled. Accordingly, the highest concentrations of these gases should indicate the hottest parts of the system.

It is evident that the lowest H_2 concentrations are calculated in the south area. The cause could be related with the boiling process or steam loss from the fluid into wells TR17 and TR17B. Both gases

H_2 and H_2S partition into the vapour phase; however, due to the lower solubility of H_2 in liquid water, H_2 is more sensitive to the presence of a vapour phase than H_2S and is considered a more reliable indicator of the equilibrium vapour fraction. H_2S and H_2 are generated by reactions with the rock that can bring their concentrations back into equilibrium after degassing has occurred.

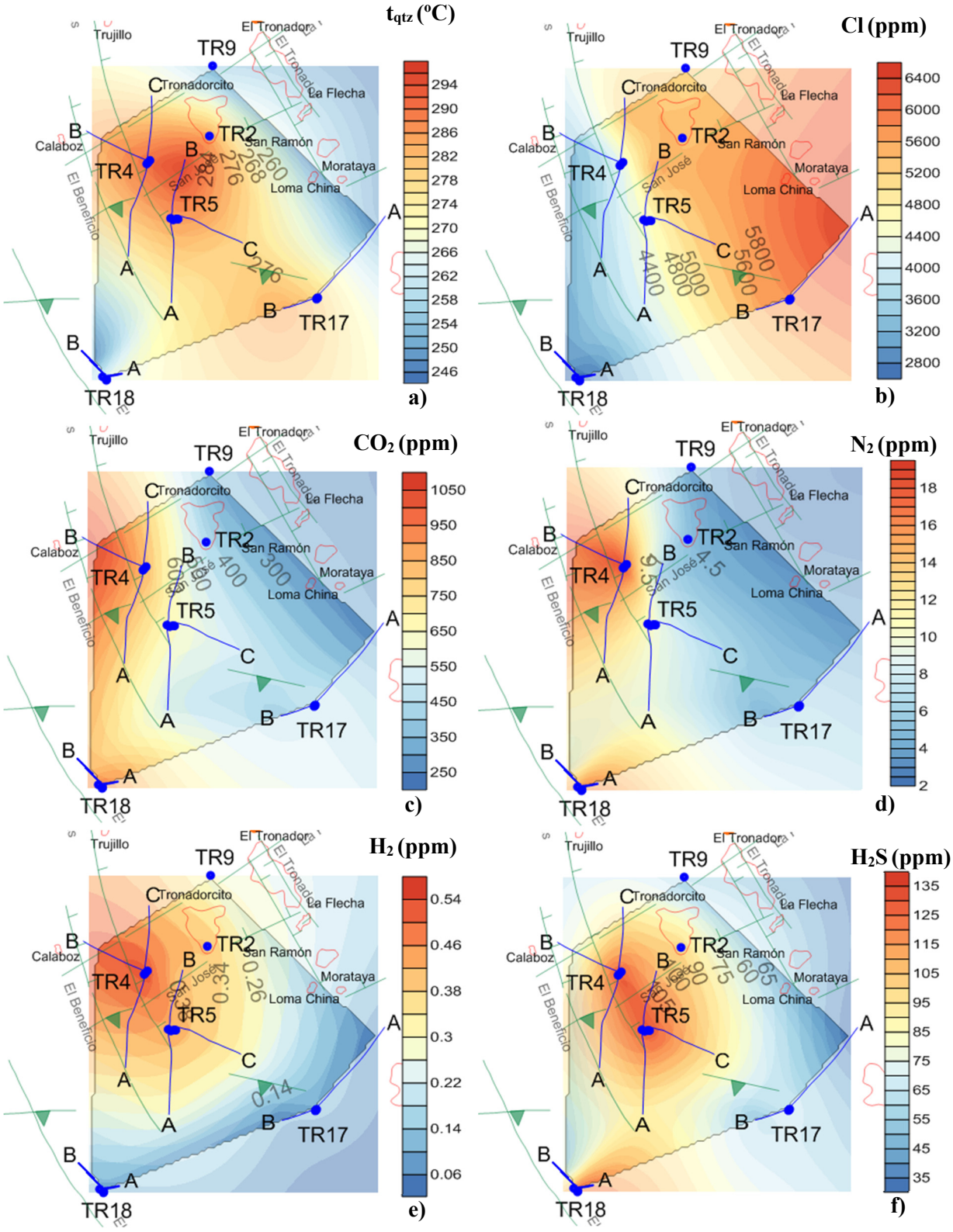

FIGURE 6: Field-scale distribution of temperature based on: (a) quartz geothermometer; (b) concentration of Cl; (c) CO_2; (d) N_2; (e) H_2; and (f) H_2S throughout the Berlín geothermal field

TABLE 10: Calculated chemical composition of the initial liquid phase in the aquifer feeding production wells at the Berlín geothermal field

Sample	Well	Discharg enthalpy kJ/kg	Aquifer temp. °C[a]	Liquid phase (mg/kg)																Chemical species (log mol)		
				pH[b]	SiO_2	B	Na	K	Mg	Ca	Al	Fe	F	Cl	SO_4	CO_2[c]	H_2S	H_2	CH_4	N_2	H_2CO_3[d]	H_2S	H_2
2013-1388	TR-2	1171	284	4.98	565	89	2933	517	0.07	89	0.48	0.09	0.39	5336	11.1	415	98	0.39	0.64	4.5	-2.03	-2.54	-3.71
2013-1373	TR-4	1291	288	5.54	578	70	2370	437	0.01	43	0.35	0.01	0.75	3993	11.2	862	130	0.53	0.86	19.4	-1.71	-2.43	-3.58
2013-1374	TR-4B	1316	281	5.80	558	63	1868	376	0.01	25	0.58	0.01	0.58	3308	9.6	1066	64	0.48	0.67	15.0	-1.62	-2.74	-3.62
2013-1375	TR-4C	1290	275	5.46	537	96	3079	535	0.02	112	0.58	0.02	0.53	5676	15.5	762	93	0.40	0.65	11.3	-1.77	-2.57	-3.70
2013-1164	TR-5	1278	282	5.07	563	88	2714	546	0.05	44	0.33	0.02	0.37	4619	8.8	615	127	0.41	0.64	8.8	-1.86	-2.43	-3.69
2013-1378	TR-5A	1216	272	5.50	527	77	2343	424	0.03	48	0.24	0.52	0.59	4273	14.7	461	86	0.28	0.50	8.5	-1.98	-2.60	-3.86
2013-1379	TR-5B	1182	295	5.27	598	103	3101	561	0.09	102	0.23	0.50	0.45	5825	9.7	563	98	0.35	0.61	4.2	-1.89	-2.54	-3.76
2013-1163	TR-5C	1193	275	4.95	540	105	2966	566	0.09	105	0.50	0.05	0.50	5419	9.8	507	93	0.31	0.55	6.1	-1.94	-2.57	-3.81
2013-1380	TR-9	1189	247	5.52	445	82	2669	418	0.01	134	0.55	0.03	0.70	5051	19.2	257	53	0.24	0.39	3.1	-2.24	-2.82	-3.92
2013-1389	TR-17	1141	277	5.07	543	97	3233	556	0.12	143	0.17	0.17	0.60	5774	7.7	510	70	0.10	0.05	5.8	-1.94	-2.69	-4.30
2013-1390	TR-17A	1156	244	5.58	434	103	3496	520	0.13	229	0.28	0.08	0.97	6406	21.4	197	32	0.02	0.02	2.9	-2.36	-3.05	-5.00
2013-1391	TR-17B	1101	281	5.50	557	98	3068	506	0.11	161	0.15	0.55	0.70	5674	13.4	369	48	0.02	0.01	3.6	-2.08	-2.86	-5.00
2013-1407	TR-18	1168	268	5.90	516	68	1500	246	0.01	27	0.79	0.03	0.61	2598	19.8	974	138	0.07	0.08	17.5	-1.66	-2.41	-4.46
2013-1408	TR-18B	1693	238	5.03	477	78	1816	315	0.01	67	0.00	0.00	3.31	3216	16.8	777	43	0.20	0.03	6.9	-1.76	-2.90	-4.00
2013-1182	TR-18B	1822	249	5.19	575	91	2260	369	0.27	142	2.81	1.02	4.63	4040	24.4	244	32	0.07	0.02	2.1	-2.26	-3.04	-4.46
2013-1208	TR-18B	1748	244	5.16	545	103	2126	382	0.17	121	1.78	0.52	0.00	4050	25.5	254	50	0.07	0.02	4.4	-1.99	-2.84	-4.46
2013-1236	TR-18B	1680	235	4.89	437	82	1933	309	0.01	82	1.06	0.02	3.68	3272	22.5	1493	78	0.47	0.05	14.2	-1.47	-2.65	-3.63
2013-1244	TR-18B	1472	238	4.92	456	83	1979	330	0.00	83	0.88	0.12	4.13	3480	22.4	1118	68	0.35	0.04	10.3	-1.60	-2.71	-3.76
2013-1250	TR-18B	1489	241	4.95	472	75	1962	325	0.00	79	0.86	0.08	3.74	3423	21.8	1116	59	0.38	0.03	9.5	-1.60	-2.77	-3.72
2013-1409	TR-18B	1693	237	5.00	470	86	1790	315	0.01	67	0.00	0.00	2.89	3264	17.4	829	44	0.17	0.02	5.4	-1.73	-2.89	-4.07
2013-1549	TR-18B	1150	234	5.00	451	85	1935	327	0.04	70	0.00	0.00	2.82	3460	21.4	950	46	0.29	0.03	8.4	-1.67	-2.88	-3.84
2014-0066	TR-18B	1653	241	5.03	490	80	1973	340	0.00	71	0.00	0.00	3.06	3444	22.9	991	43	0.28	0.03	8.9	-1.65	-2.91	-3.86
2014-0217	TR-18B	1652	241	5.13	491	92	1995	349	0.00	72	0.00	0.00	2.86	3417	25.2	902	40	0.20	0.02	6.5	-1.69	-2.94	-4.00
2014-0360	TR-18B	1652	240	5.02	485	78	1860	297	0.00	66	0.00	0.00	3.28	3335	20.8	1219	43	0.36	0.04	11.4	-1.56	-2.90	-3.75
2014-0891	TR-18B	1676	235	5.02	485	78	1860	297	0.00	66	0.00	0.00	3.28	3335	20.8	1219	43	0.36	0.04	11.4	-1.62	-2.91	-3.75

[a]: temperature based on quartz geothermometer (Gudmundsson and Arnórsson, 2002) [b]: pH at aquifer temperature reported in the column to the left
[c]: total carbonate carbon as CO_2 [d]: used as aquifer water CO_2 concentrations in mineral assemblage-gas equilibria

4.2 Mineral assemblages

Secondary minerals such as epidote and albite, which coexist with quartz, illite, chlorite, calcite, wairakite, adularia and prehnite, are found in drill cuttings from Berlín geothermal field. In several samples, minor amounts of titanite and pyrite are also observed without clear depth distribution (Rugierri et al., 2006).

One difficulty in making the determination of which mineral assemblage is involved in controlling the gas concentrations in the geothermal fluid is that the equilibrium concentrations of gases predicted by different possible mineral buffers fall within a narrow range, even within the range of uncertainty inherent in the process of fluid sampling and analysis. Additionally, different mineral assemblages have been identified to control reactive gas concentrations in geothermal fields of different geological settings (Scott, 2011). However, Arnórsson et al. (2007) pointed out that some of the different mineral assemblages give very similar aqueous H_2S, H_2 and CO_2 equilibrium concentrations when the end member activities of the solid solution minerals are properly chosen.

The equilibrium curves of the mineral assemblages that could potentially fix the concentrations of the reactive gases H_2S, H_2 and CO_2 in the Berlín geothermal field (reactions 1-10, Table 10) are plotted in Figure 7, in the temperature range 200 to 300°C and at the selected mineral compositions (a_{epi}=0.72, a_{czo}=0.28, a_{pre}=0.66, a_{gro}=0.3).

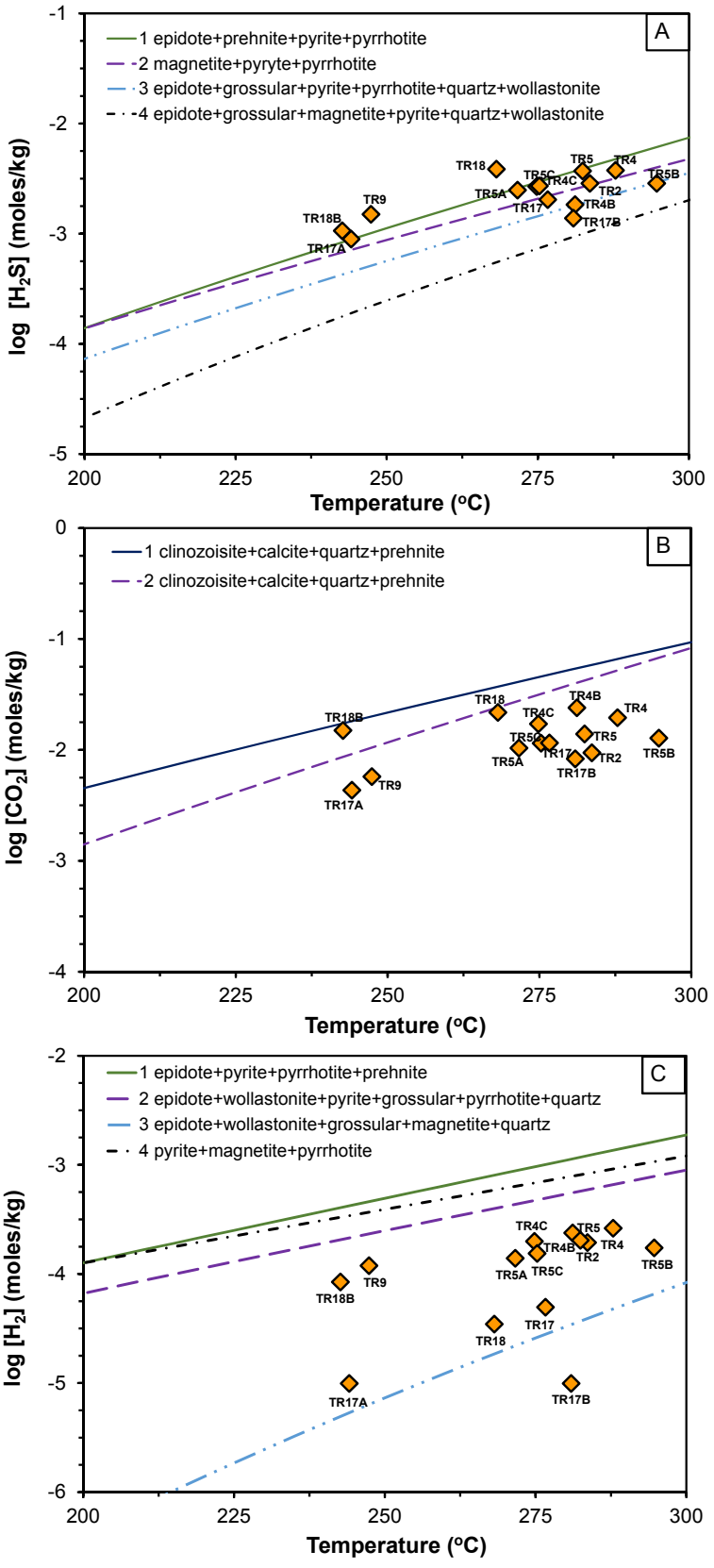

FIGURE 7: Mineral buffer reaction equilibrium between dissolved (a) H2S, (b) CO2 and (c) H_2 in the aquifer liquid of production wells of Berlín geothermal field

The activity of the H_2S species for the fluids in Berlin geothermal field are shown in Figure 7a. At the selected mineral compositions, it is difficult to distinguish between which of the 3 mineral

assemblages control the gas concentrations, because the equilibrium gas concentrations given by the different mineral assemblages are quite similar throughout the temperature range of interest; the concentrations given by mineral buffer 1 (epi-pre-pyr-pyrr) and buffer 2 (mag-pyr-pyrr) mineral assemblages differ by only 0.13 to 0.29 log units. However, if considering that the H_2S data randomly moved around the equilibrium curves, mineral buffers 1 (epi-pre-pyr-pyrr) and 3 (epi-gro-pyr-pyrr-qtz-wol) seem to be more probable. The concentration of H_2S in Berlin geothermal field does, however, clearly indicate a temperature control.

Concentration of the CO_2 species in Berlin geothermal field is shown in Figure 7b. The CO_2 species concentration for some wells lies close to the equilibrium line for the mineral assemblage used in this study, but there seems to be no clear temperature trend. The concentrations seem to be constant for the temperature range of the Berlin field. One explanation for this is that the CO_2 concentration is not, in fact, controlled by equilibrium with a mineral assemblage but is rather source-controlled. CO_2 concentration in the field-scale distribution appears to follow a similar pattern as that of N_2, which is generally known to be source controlled.

Concentration of H_2 (Figure 7c) in the Berlin field seems to be in two categories. All data points, except for wells TR17, TR17A, TR17B and TR18, seem to align in a temperature controlled relationship although they are not very close to the equilibrium lines shown in Figure 7c; wells TR17, TR17A, TR17B and TR18 seem to be depleted of H_2 when compared to the rest of the wells. These depleted wells are all wells on the south side of the production field.

If considering mineral assemblage 3 (epi-wol-gro-mag-qtz), the relatively large stoichiometric coefficients in reaction (10) of Table 9 show that the equilibrium aqueous concentrations of H_2 are strongly affected by the compositions of grossular garnet. Figure 8 illustrates how variable compositions of grossular garnet affect the equilibrium curves of this reaction. Equilibrium gas concentrations given by the other mineral assemblages in Figure 7c assume unit activity, for all the minerals are not significantly affected by adjusting the curve for activities of the solid-solution minerals prehnite and epidote.

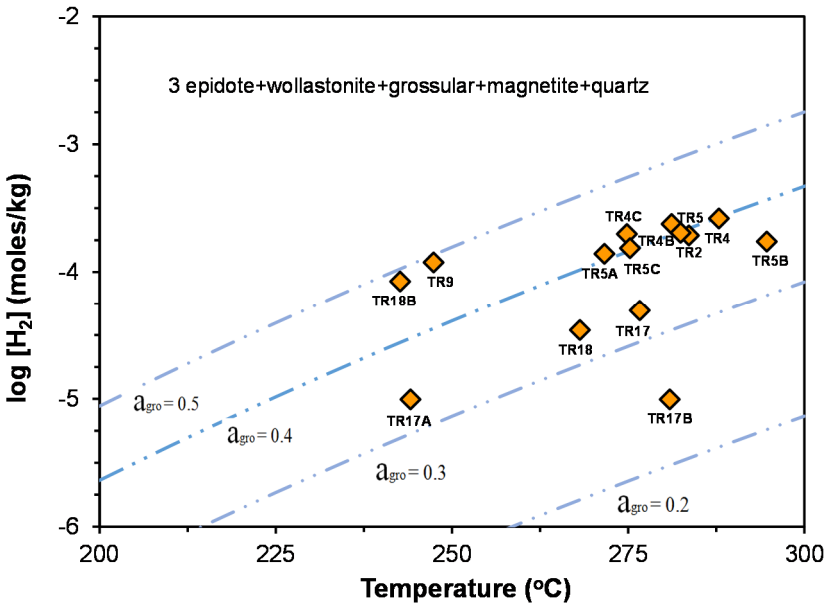

FIGURE 8: Mineral buffer reaction equilibrium between dissolved H_2 and mineral assemblages considered by reaction 10 in Table 9, at variable compositions of grossular

Hydrogen concentration for most of the wells (TR5, TR5A, TR5C, TR2, TR4, TR4B and TR4C) lies close to the equilibrium line, using compositions of a grossular value of 0.4 (a_{gro}=0.4), while wells TR18B and TR9 closely approach equilibrium with the mineral assemblages using a_{gro}=0.5. Angcoy (2010) concluded that the H_2 concentrations in the silicic volcanic of the Mahanagdong geothermal field in the Philippines best corresponded to the epi-wol-gro-mag-qtz mineral assemblage.

As mentioned before, wells of the north zone (TR17, TR17A, TR17B and TR18) are depleted in H_2. A possible explanation for this is that they represent waters that have not equilibrated yet due to short reaction times in the geothermal reservoir. Scott (2011) concluded that apparent H_2 depletion in well fluids on the edges of Hellisheidi geothermal field, Iceland, was a result of insufficient equilibrium time.

5. SUMMARY AND CONCLUSIONS

This study is based on the results of the calculation of aquifer fluid composition at depth of the volcanic geothermal system of Berlín, El Salvador, using chemical speciation program WATCH 2.4 and chemical data from water and steam discharge samples collected and analysed by geochemical laboratory of LaGeo from 14 currently producing wet-steam wells. All fluids were sampled during the period from July to October 2013, except for samples collected from well TR18B which was sampled during the period from July 2013 to July 2014.

All the well discharges have liquid enthalpy (i.e. the enthalpy of the discharged fluid is equal, or very close, to the enthalpy of steam-saturated liquid at the aquifer temperature) except for well TR18B. The evaluation of initial aquifer fluid compositions for wells with liquid enthalpy were calculated according to a model where the depth level of first boiling is within the well and the thermodynamic system is considered an isolated system.

It was shown that the process of phase segregation, caused by the retention of liquid onto mineral grain surfaces, best accounts for the observed decreasing concentrations of Cl in the total well discharge with an increase in discharge enthalpy; similarly, evaluation of the relationship between Na/K and quartz geothermometers suggests that the main cause of elevated discharge enthalpy is caused by phase segregation in the depressuration zone around the well. Modelling of aquifer fluid compositions using the phase segregation model was applied to well TR18B.

The chemical composition of the deep water reservoir in the Berlín geothermal field indicated that the reservoir is liquid-dominated and sub-boiling at depth with an aquifer fluid temperature based on a quartz geothermometer in the range of 240-285°C in the south, and from 275 to 300°C in the central and northeast zones. Field-scale distribution of the concentration of selected gases, in the initial aquifer fluid in the production zone of the Berlín geothermal field, shows that H_2S and H_2 appear to follow similar patterns as indicated by the quartz geothermometer. This indicates that the concentrations of gases are temperature controlled, whereas CO_2 appears to follow a similar pattern as N_2, which is generally known to be source controlled in geothermal systems.

The concentration of the H_2S species is clearly controlled by close approach to equilibrium with mineral assemblages known to actively control H_2S species concentration in geothermal systems (Angcoy, 2010; Arnórsson et al., 2007, 2010; Karingithi et al., 2010; Scott, 2011). However, considering that the H_2S species concentration randomly scatters around the equilibrium curves of at least three mineral assemblages, it is difficult to ascertain which of the 3 mineral assemblages controls the gas concentration. Equilibrium gas concentrations given by the different mineral assemblages are quite similar throughout the temperature range of interest.

The concentration of H_2 seems to be in two categories: most of the wells seem to be controlled by a close approach to equilibrium with respect to a mineral assemblage consisting of epidote-wollastonite-grossular-magnetite-quartz, except for wells TR17, TR17A, TR17B and TR18. These wells seem to be depleted in H_2 in comparison with the rest of wells. The depletion in H_2 in wells TR17, TR17A, TR17B and TR18, when compared to others, could indicate insufficient equilibrium time for the recharging geothermal fluids.

ACKNOWLEDGEMENTS

This is a great chance to express my sincere thanks to the United Nations University Geothermal Training Program and the Government of Iceland for granting me the opportunity to be a fellow in this excellent program. Special thanks go to the director of the UNU-GTP, Mr. Lúdvík S. Georgsson, and to Ms. Thórhildur Ísberg, Mr. Ingimar G. Haraldsson, Mr. Markús A. G. Wilde and Ms. Málfrídur Ómarsdóttir for their assistance throughout these six months and for making every fellow feel welcome in Iceland.

I would like to express my appreciation to my employer, LaGeo S.A. de C.V. for allowing me to participate in UNU-GTP, to my boss, Roberto Renderos, for his trust and support, and to all my colleagues at the Geochemical Laboratory and Studies Department for their valuable assistance and help during my project.

Special thanks to Thráinn Fridriksson for his excellent work and guidance throughout the chemistry specialization course. Thanks to all other ÍSOR staff and lecturers. Sincere thanks to my supervisor, Ingvi Gunnarsson, for being an outstanding guide and for his extra effort and time spent trying to understand my "fancy" English. Certainly this report could not have been completed without his guidance and input.

I say thank you to all 2014 UNU Fellows, especially to the Chemistry or Landspítali group: Melissa, Yid, Melese, Edwin, Leakey, and Daniel "teschemacherite" Villarroel for their company, fruitful discussions and fun times during these six months in Iceland.

I would also like to take this opportunity to thank my family and my wife for giving me moral support, love, prayers and encouragement. Finally, I want to thank God for good health, strength and his blessings during my stay in Iceland.

REFERENCES

Angcoy Jr., E.C., 2010: *Geochemical modelling of the high-temperature Mahanagdong geothermal field, Leyte, Philippines*. University of Iceland, MSc thesis, UNU-GTP, report 1, 79 pp.

Arnórsson, S. (ed.), 2000: *Isotopic and chemical techniques in geothermal exploration, development and use. Sampling methods, data handling, interpretation*. International Atomic Energy Agency, Vienna, 351 pp.

Arnórsson, S., 2008: Chemical thermodynamics of two-phase geothermal systems. International Conference on the Properties of Water and Steam, Berlin, Germany.

Arnórsson, S., and Stefánsson, A., 2005a: Wet-steam well discharges. I. Sampling and calculation of total discharge compositions. *Proceedings of the World Geothermal Congress 2005, Antalya, Turkey*, 8 pp.

Arnórsson, S., and Stefánsson, A., 2005b: Well-steam well discharges II. Assessment of aquifer fluid compositions. *Proceedings of the World Geothermal Congress 2005, Antalya, Turkey*, 11 pp.

Arnórsson, S., Stefánsson, A., and Bjarnason, J.Ö., 2007: Fluid-fluid interaction in geothermal systems. *Rev. Mineralogy & Geochemistry, 65*, 229-312.

Arnórsson, S., Sigurdsson, S. and Svavarsson, H., 1982: The chemistry of geothermal waters in Iceland I. Calculation of aqueous speciation from 0°C to 370°C. *Geochim. Cosmochim. Acta, 46,* 1513-1532.

Arnórsson, S., Andrésdóttir, A., Gunnarsson, I., and Stefánsson, A., 1998: New calibration for the quartz and Na/K geothermometers – valid in the range 0-350ºC (in Icelandic). *Proceedings of the Geoscience Society of Iceland Annual Meeting, April,* 42-43.

Arnórsson, S., Angcoy Jr., E.C., Bjarnason, J.Ö., Giroud, N., Gunnarsson, I., Kaasalainen, H., Karingithi, C., and Stefánsson, A., 2010: Gas chemistry of volcanic geothermal systems. *Proceedings of the World Geothermal Congress 2010, Bali, Indonesia,* 12 pp.

Axelsson, G., 2013: Conceptual models of geothermal systems – Introduction. *Presented at "Short Course V on Conceptual Modelling of Geothermal Systems", UNU-GTP and LaGeo, Santa Tecla, El Salvador,* 12 pp.

Barrios, L., Hernández, B., Quezada, A., and Pullinger, C. 2011: Geological hazards and geotechnical aspects in geothermal areas, the El Salvador experience. *Presented at "Short Course on Geothermal Drilling in Central America – Resource Development and Power Plants", UNU-GTP and LaGeo, Santa Tecla, El Salvador,* 14 pp

Bjarnason, J.Ö., 2010: *The speciation program WATCH* (vers. 2.4). ISOR – Iceland GeoSurvey, Reykjavík.

Correia, H., Jacobo, H., Castellanos, F., Tenorio, J., Handal, S., and Santos, P., 1996: *Synthesis of geoscientific information of a conceptual model of Berlín geothermal field.* Internal report, CEL, El Salvador, 30 pp.

D'Amore, F., and Tenorio, J., 1999: Chemical and physical reservoir parameters at initial conditions in Berlín geothermal field, El Salvador: A first assessment. *Geothermics, 28*, 45-73.

Fournier, R.O., and Truesdell, A.H., 1973: An empirical Na-K-Ca geothermometer for natural waters. *Geochim. Cosmochim. Acta*, *37*, 1255-1275.

Freedman, A. J.E., Bird, D.K., Arnórsson, S., Fridriksson, Th., Elders, W.A., Fridleifsson, G.Ó., 2010: Hydrothermal mineral record CO_2 partial pressures in Reykjanes geothermal system, Iceland. *Proceedings of the World Geothermal Congress 2010, Bali, Indonesia*, 11 pp.

Giroud, N., 2008: *A chemical study of arsenic, boron and gases in high-temperature geothermal fluids in Iceland.* University of Iceland, Faculty of Science, PhD thesis, 110 pp.

Gudmundsson, B.T. and Arnórsson, S., 2002: Geochemical monitoring of the Krafla and Námafjall geothermal areas, N-Iceland. *Geothermics, 31,* 195-243.

Hernández M., C.B., 2012: Aquifer fluid compositions at the Berlín geothermal field, El Salvador in 2012. Report 12 in: *Geothermal training in Iceland 2012*.UNU-GTP, Iceland, 169-202.

Jacobo, P., 2003: Gas chemistry of the Ahuachapán and Berlín geothermal fields, El Salvador, Report 12 in: *Geothermal Training in Iceland 2003*. UNU-GTP, Iceland, 275-304.

Karingithi, C.W., Arnórsson, S., and Grönvold, K., 2010: Processes controlling aquifer fluid compositions in the Olkaria geothermal system, Kenya. *J. Volc. & Geotherm. Res., 196,* 57-76

LaGeo, 2012: *Conceptual model of the Berlín geothermal system*. LaGeo S.A. de C.V., Studies and Production Departments, internal report (in Spanish), 143 pp.

Magaña, M.I., 2012: *Geochemical model. Berlín geothermal system*. LaGeo S.A de C.V., Geochemical Department, internal report (in Spanish), 21 pp.

Montalvo, F., and Axelsson, G., 2000: Assessment of chemical and physical reservoir parameters during six years of production-reinjection at Berlín geothermal field (El Salvador). *Proceedings of the World Geothermal Congress 2000, Kyushu-Tohoku, Japan,* 2153-2158.

Monterrosa, M., and Santos, P., 2013: Conceptual models for the Berlín geothermal field, Case history. *Presented at "Short Course V on Conceptual Modelling of Geothermal Systems", UNU-GTP and LaGeo, Santa Tecla, El Salvador,* 9 pp.

Raymond, J., Williams-Jones, A.E., and Clark, J.R., 2005: Mineralization associated with scale and altered rock and pipe fragments from the Berlín geothermal field, El Salvador; implications for metal transport in natural systems, *J. Volcanology & Geothermal Research, 145*, 81-96.

Renderos, R., 2002: Chemical characterization of the thermal fluid discharge from well production tests in the Berlín geothermal field, El Salvador. Report 12 in: *Geothermal Training in Iceland 2002*. UNU-GTP, Iceland, 205-232.

Ruggieri, G., Dallai, L., Nardini, I., Henriquez, E.T., and Arias, A., 2010: Thermo-chemical variations of the hydrothermal fluids in the Berlin geothermal field (El Salvador). *Proceedings of the World Geothermal Congress 2010, Bali, Indonesia*, 7 pp.

Ruggieri, G., Petrone, C.M., Gianelli, G., Arias, A., and Henriquez, E.T., 2006: Hydrothermal alteration in the Berlin geothermal field (El Salvador): new data and discussion on the natural state of the system. *Periodico di Mineralogia, 75*, 347-353.

Saemundsson, K., 2009: Geothermal systems in global perspective. *Presented at "Short Course IV on Exploration for Geothermal Resources", UNU-GTP, KenGen and GDC, Lake Naivasha, Kenya,* 11 pp.

Scott, S., 2011: *Gas chemistry of the Hellisheidi geothermal field.*University of Iceland, MSc thesis, 63 pp.

Truesdell, A.H., 1976: Summary of section III - geochemical techniques in exploration. *Proceedings of the 2nd U.N. Symposium on the Development and Use of Geothermal Resources, San Francisco, 1,* liii-lxxix.

Zhen-Wu, B.Y., 2010: Gas geochemistry of the Miravalles, Pailas and Borinquen geothermal areas of Costa Rica, and a comparison with Reykjanes and Theistareykir geothermal fields, Iceland. Report 33 in: *Geothermal Training in Iceland 2010*. UNU-GTP, Iceland, 731-766.